DOT/FAA/AR-02/99

Office of Aviation Research
Washington, D.C. 20591

Development of a Component Head Injury Criteria (HIC) Tester for Aircraft Seat Certification—Phase I

November 2002

Final Report

U.S. Department of Transportation
Federal Aviation Administration

NOTICE

Technical Report Documentation Page

1. Report No.	2. Government Accession No.	3. Recipient's Catalog No.
DOT/FAA/AR-02/99		

4. Title and Subtitle	5. Report Date
DEVELOPMENT OF A COMPONENT HEAD INJURY CRITERIA (HIC) TESTER FOR AIRCRAFT SEAT CERTIFICATION—PHASE I	November 2002
	6. Performing Organization Code

7. Author(s)	8. Performing Organization Report No.
Hamid Lankarani	

9. Performing Organization Name and Address	10. Work Unit No. (TRAIS)
National Institute for Aviation Research Wichita State University 1845 N. Fairmount Wichita, KS 67260-0093	11. Contract or Grant No. 00-C-WSU - 00 Amendment Number 4

12. Sponsoring Agency Name and Address	13. Type of Report and Period Covered
U.S. Department of Transportation Federal Aviation Administration Office of Aviation Research Washington, DC 20591	Final Report From 08/00 to 09/01
	14. Sponsoring Agency Code ANM-106

15. Supplementary Notes

Program Manager: Gary Frings, Federal Aviation Administration, William J. Hughes Technical Center
Technical Monitor: Dr. Tong Vu, Federal Aviation Administration, William J. Hughes Technical Center.

16. Abstract

Compliance with head injury criteria (HIC) poses a significant problem for the airlines due to claims of high costs incurred during the development and certification of aircraft seats. One problem encountered in the certification of 16-g airline seats occurs for seats located directly behind bulkheads or cabin class dividers. This research addresses the development of an alternate component testing method for the evaluation of HIC without consuming a seat during each test. The component HIC testing device can be used to evaluate different designs and test conditions at relatively low cost and in a short period of time. This device may be used to identify critical impact parameters. This report contains the design, fabrication, and calibration of the component HIC device.

17. Key Words	18. Distribution Statement
Aircraft crashworthiness, Head injury criteria, HIC, Component tester	This document is available to the public through the National Technical Information Service (NTIS) Springfield, Virginia 22161.

19. Security Classif. (of this report)	20. Security Classif. (of this page)	21. No. of Pages	22. Price
Unclassified	Unclassified	69	

TABLE OF CONTENTS

LIST OF FIGURES

LIST OF TABLES

EXECUTIVE SUMMARY

One problem in the certification of 16-g airline seats, referred to as the front-row head injury criteria (HIC) problem, occurs for seats located directly behind bulkheads or cabin class dividers. These structures are typically both stiff and strong and, therefore, produce very high HIC values during head impacts. Currently, several full-scale sled tests (FSSTs) are conducted to determine the HIC value, during which the seats used are usually destroyed, resulting in significant costs. In addition, inherent variations in the dynamic environment of the sled tests may result in HIC data scatter.

The airline industry has made claims of high costs and significant schedule overruns during the development and certification of 16-g seats because of the difficulties encountered in meeting this requirement. In many cases, the airlines have removed one row of seating in order to address this problem, resulting in loss of revenue.

The objective of this research project was to develop a component test apparatus that effectively supports the design and certification of aircraft seats to meet the HIC requirements. This device will minimize the need for FSSTs and reduce the associated time and costs for development and certification of aircraft seats.

The National Institute for Aviation Research has designed, fabricated, and performed preliminary evaluations of an alternative HIC component tester (HCT).

Results from the HCT have been compared to test results from full-scale sled tests. Comparisons were based on the head impact angle, head impact velocity, HIC, HIC window, peak head center of gravity (c.g.) resultant acceleration, average head c.g. resultant acceleration, and head c.g. resultant acceleration profiles. The comparisons were performed for both modes of operation of the HCT using aluminum type bulkheads and Nomex honeycomb type bulkheads.

For the aluminum type bulkhead, the HIC, HIC window, and peak average head c.g. resultant acceleration showed good agreement. However, the head c.g. resultant acceleration profiles did not. The HCT showed repeatability for both modes. The results for both modes of operation were similar.

For the Nomex honeycomb type bulkhead, the HIC, HIC window, and peak average head c.g. resultant acceleration showed little agreement. The resultant acceleration profiles show poor agreement. The HCT showed repeatability for Mode I. A repeatability test was not conducted for Mode II. The results for both modes of operation were similar.

1. INTRODUCTION.

One problem in the certification of 16-g airline seats, referred to as the front-row head injury criteria (HIC) problem, occur for seats located directly behind bulkheads or cabin class dividers. These structures are typically both stiff and strong and, therefore, produce very high HIC values during head impacts. Currently, several full-scale sled tests (FSSTs) are conducted to determine the HIC value, during which the seats used are usually destroyed. In addition, inherent variations in the dynamic environment of the sled tests may result in HIC data scatter.

The airline industry has made claims of high costs and significant schedule overruns during the development and certification of 16-g seats because of the difficulties encountered in meeting this requirement. In many cases, the airlines have removed one row of seating in order to address this problem, resulting in loss of revenue.

The objective of this research was to develop a component test apparatus that effectively supports the design and certification of aircraft seats to meet the HIC requirements. This device will minimize the need for full-scale tests and reduce the associated time and costs for aircraft seat development and certification.

2. BACKGROUND.

Chandler [1] described development of the head injury criteria. This injury criterion evolved from the Wayne State Tolerance Curve [2]. Gadd [3] defined the severity index (SI) based on raising the time integral of head acceleration in g's to the power of 2.5, after observing this to be the slope of the line which closely fit the Wayne State data when it was plotted using a log-log scale. Gadd also proposed the injury threshold of 1000. Versace [4] subsequently advocated the use of an effective acceleration, which he defined as

$$\left\{ {}^{1}\!/_{t} \int a^{2.5}\, dt \right\}$$

where t and a respectively represent the time interval and resultant head acceleration. The head injury criteria, HIC, was subsequently defined by Gurdjian [5 and 6] as

$$\mathrm{HIC} = \left[(t_2 - t_1) \left\{ \frac{1}{(t_2 - t_1)} \int_{t_1}^{t_2} a(t)dt \right\}^{2.5} \right]_{\max}$$

where:

$a(t)$	=	resultant acceleration of the head center of gravity in g's
t_1	=	initial integration time, expressed in seconds
t_2	=	final integration time, expressed in seconds

A maximization is performed by identifying the time interval $t_2 - t_1$ that results in the largest functional value. This criterion was adapted from the Federal Motor Vehicle Safety Standard (FMVSS) No. 208 [7].

In aerospace applications, the HIC is evaluated over the period when the head of the anthropomorphic test dummy (ATD) is in contact with any structure on the aircraft interior. Injury is defined as any HIC value exceeding the threshold value of 1000. The HIC was subsequently recommended as one of the injury criteria by the General Aviation Safety Panel (GASP) to be considered in the design and certification of aircraft seats and restraint systems. HIC requirements were adapted and are specified in Title 14 Code of Federal Regulations (CFR) 23.562 [8] and 14 CFR 25.562 [9].

Alternative methods involving the use of component test devices represent useful engineering tools for HIC evaluation in both the aircraft and automotive industry. A validated component test device should be simple to use, operate, and control. The device should show good repeatability and produce less data scatter than that obtained from an FSST. Validation of a HIC component tester requires that the measurements of the following parameters from component tests agree with the values of the corresponding parameters acquired from FSSTs.

- HIC
- HIC window, $\Delta t = t_2 - t_1$
- Average head c.g. resultant acceleration
- Head c.g. resultant acceleration profile

There are several component testers that were developed primarily. A detailed description of each device listed is given in appendix A.

- Bowling Ball Tester
- Free Motion Headform Tester
- MGA Head/Neck Impactor
- Pendulum Test Rig Tester

A study of these devices determined that they do not provide adequate correlation with the FSSTs for required test conditions [10]. The component level devices provide reasonable correlation compared with the 16-g dynamic FSSTs only for configurations with predominantly normal head impact velocities, short distances from the impact surface, and relatively short duration impacts. Factors affecting these differences may include articulation of other body segments for the ATD, belt compliance, translation motion of the pelvis, and friction of the pelvic/seat and head/frontal structure. The National Institute for Aviation Research (NIAR) has developed a HIC component tester (HCT) designed to overcome the problems facing existing component testers and reproduce the test results of FSSTs of a Hybrid II (49 CFR Part 572) ATD.

3. DEVELOPMENT METHODOLOGY.

Figure 1 shows the methodology employed to design and develop the HCT.

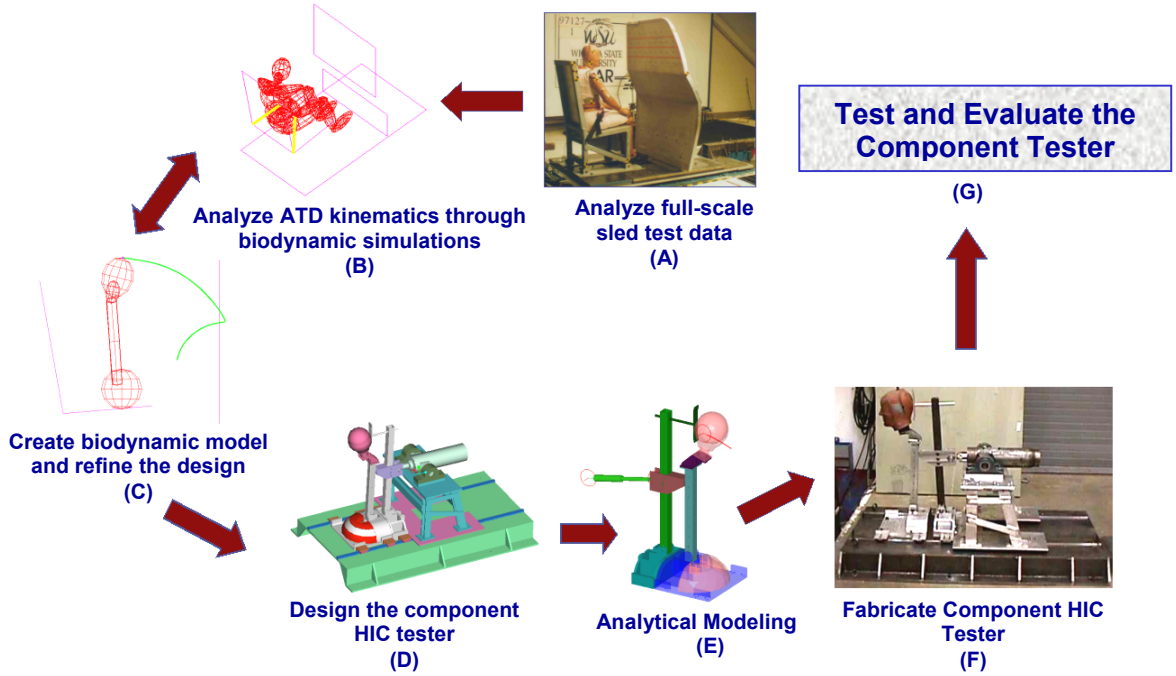

FIGURE 1. DESIGN METHODOLOGY FOR THE HIC COMPONENT TESTER

Existing FSST data from bulkhead tests conducted at NIAR, as well as HIC data provided by seat manufacturers, were analyzed and used to develop a mathematical model for biodynamic simulations (steps A and B). A biodynamic model was created, tested, and used to design a preliminary HIC component tester (PHCT). The PHCT was fabricated, tested, and refined to optimize results (step C). Using this information, the HCT was designed, tested analytically, and fabricated (steps D, E, and F). The HCT was tested, and the results were compared with FSST data (step G).

3.1 DEVELOPMENT MODELING (STEPS A AND B IN FIGURE 1).

An analytical model of the Hybrid II ATD was developed to reproduce its kinematics during a dynamic seat test. The model was validated against data obtained from FSSTs for different seat setback distances, bulkhead types, and belts [11] using biodynamic software MADYMO [12]. The purpose of developing this model was to study the kinematics and determine an initial design of a component tester, which can replicate the characteristics of an ATD during a dynamic FSST.

Figure 2 shows the kinematics of the full-scale ATD test 97191-02 and the full-scale ATD model. The kinematics of the model is in close agreement with that of the sled test.

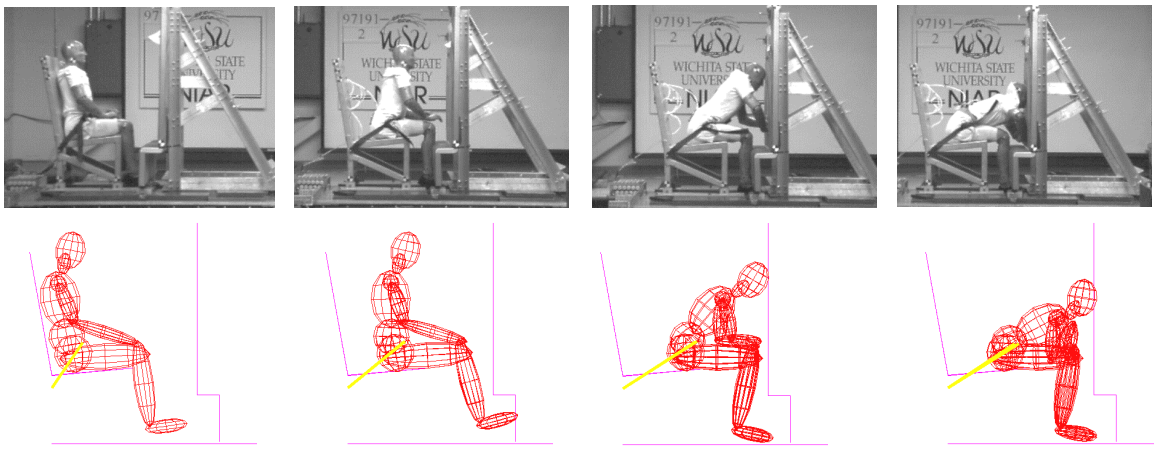

FIGURE 2. COMPARISON OF KINEMATICS OF FULL-SCALE ATD TEST 97191-02 AND FULL-SCALE ATD MODEL

The head c.g. resultant acceleration comparison for both the tests are shown in figure 3 and show good agreement.

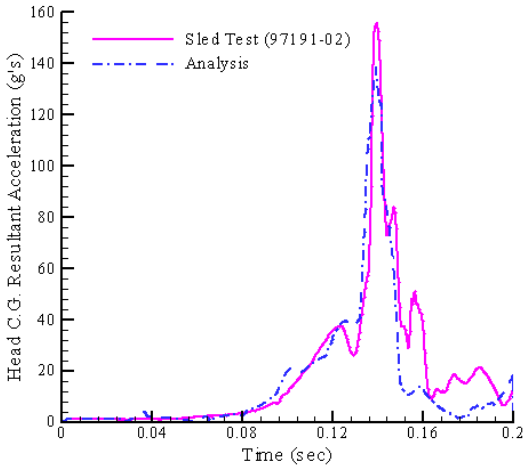

	Sled Test	Full-Scale ATD Model
HIC	1394	1343
Δt (ms)	12.5	14.2
Resultant Peak c.g. Accel. (g's)	156	139
Average Accel. (g's)	104	98

FIGURE 3. HEAD c.g. RESULTANT ACCELERATION COMPARISON OF FSST WITH A FULL-SCALE ATD MODEL

3.2 BIODYNAMIC MODELING (STEP C IN FIGURE 1).

An analytical model of the component HIC tester was developed using the full-scale Hybrid II ATD model. The purpose of this analysis was to obtain a suitable initial design for the model and to optimize its configuration by conducting parametric studies. Analyses were conducted to arrive at the final configuration that best resembles the kinematics of a belted Hybrid II ATD in a full-scale 16-g test.

Figure 4 shows the initial design of the tester model derived from the full-scale ATD model. The tester model consists of a pendulum arm representing the spine and the upper torso of the

Hybrid II ATD. The lower torso of the tester model is represented by an ellipsoid, which is equivalent to the lower torso and legs of the Hybrid II ATD. Seat reference point refers to the point formed by the intersection of planes drawn from the seat back and the seat pan. The weight distribution for the tester model was obtained from the weight distribution of the Hybrid II ATD.

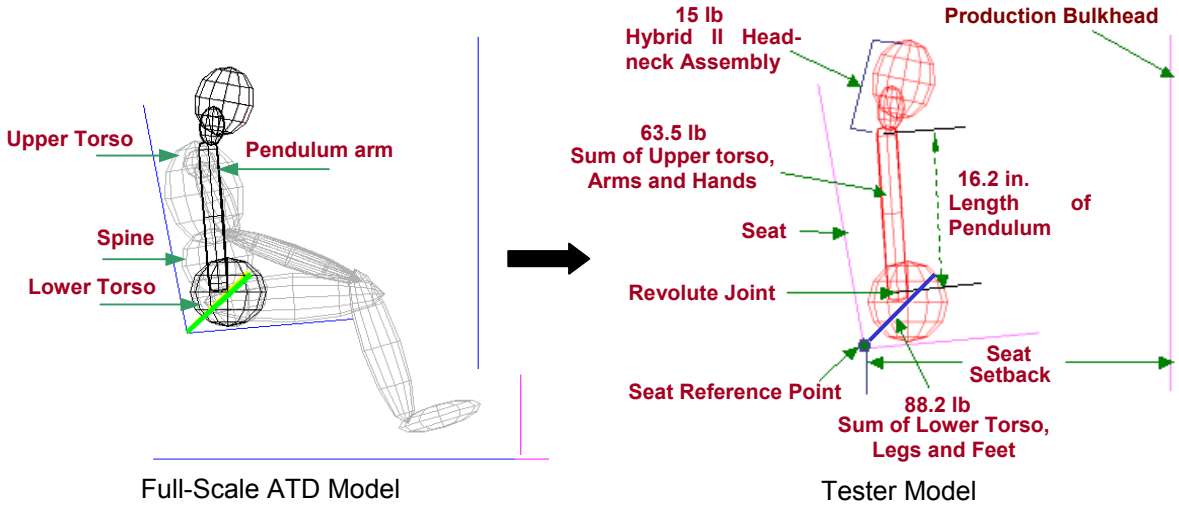

FIGURE 4. INITIAL DESIGN AND WEIGHT DISTRIBUTION OF TESTER

A mathematical model of the seat-tester-bulkhead configuration was developed in which a rigid seat is represented as two rigid planes that are fixed in space. A 50th percentile Hybrid II ATD head/neck model was used for all simulations and a rigid plane represented the bulkhead. The head orientation at the time of impact was determined using the head impact angle sign convention shown in figure 5. The representative head path of the tester model and the position at the time of impact are shown in figure 6. The seat reference point is located at the intersection of the seat back and seat pan. Seat setback distance refers to the horizontal distance from the bulkhead surface to the seat reference point. The pivot point refers to the location about which the spine/upper torso pivots about the lower torso (Revolute Joint). The pivot point setback distance refers to the horizontal distance from the bulkhead surface to the pivot point. The difference between the initial pivot point setback distance and the smallest pivot point setback distance during the FSST equals maximum belt stretch. As the point of maximum belt stretch is reached, the ATD upper torso pivots about its pelvis and impacts the bulkhead. At this point of maximum belt stretch, the head impact angle and corresponding pivot point setback distance are evaluated.

A comparison of the kinematics of the full-scale ATD model and tester model with one-degree of freedom (rotation) is shown in figure 7. As the figures indicate, both systems have similar kinematics. The head c.g. resultant acceleration comparison of the full-scale ATD model and the tester model is shown in figure 8. Examination shows good agreement between the acceleration profiles.

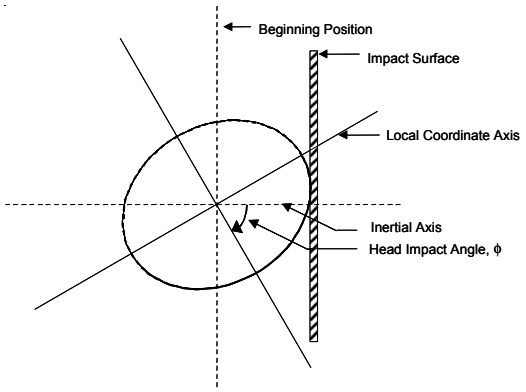

FIGURE 5. HEAD IMPACT ANGLE SIGN CONVENTION

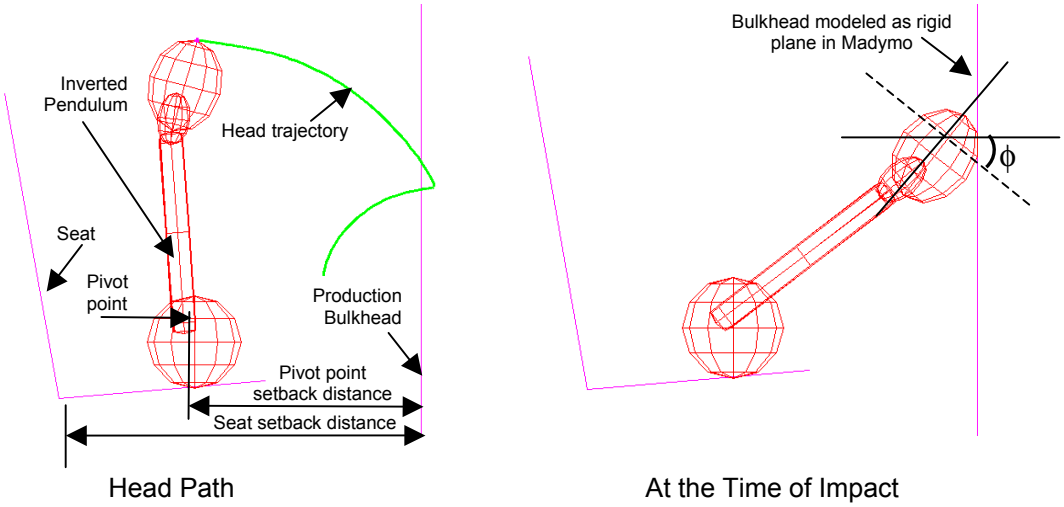

FIGURE 6. HEAD PATH AND POSITION OF TESTER AT TIME OF IMPACT

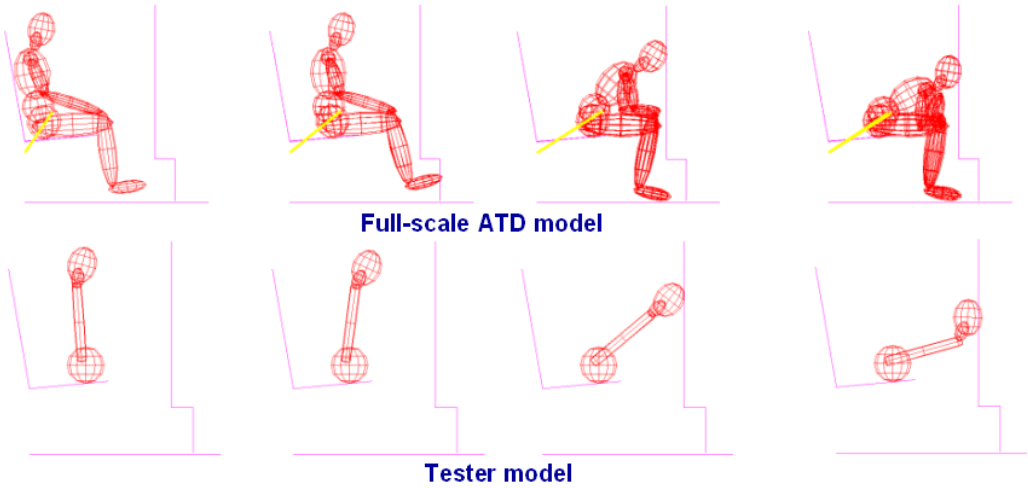

FIGURE 7. FULL-SCALE ATD MODEL AND TESTER MODEL COMPARISON

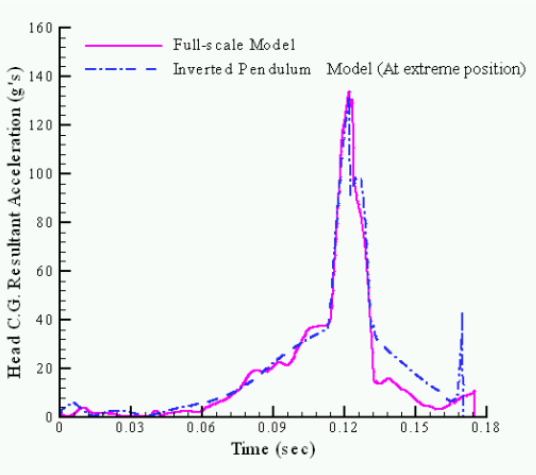

	Full-Scale ATD Model	Tester Model
HIC	1343	1338
Δt (ms)	14.2	15.0
Resultant Peak c.g. Accel. (g's)	139	132
Average Accel. (g's)	98	95

FIGURE 8. HEAD c.g. RESULTANT ACCELERATION COMPARISON OF FULL-SCALE ATD MODEL WITH TESTER MODEL

A preliminary HIC component tester (PHCT) was designed and fabricated based on the tester model. The PHCT was mounted on NIAR's rigid iron seat and tested with a simulated bulkhead fixture. The objective was to compare the PHCT results with a FSST. The PHCT model and pretest setup condition are shown in figures 9 and 10, respectively.

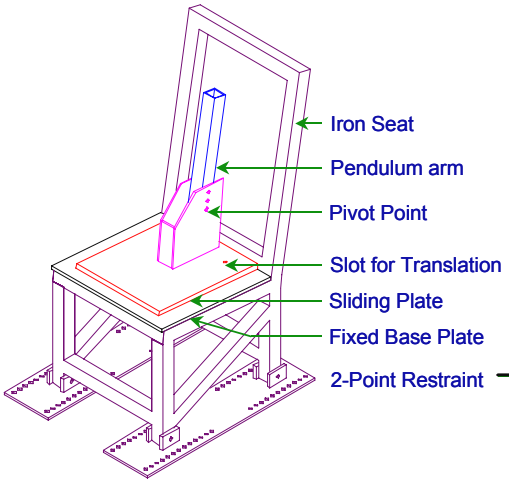

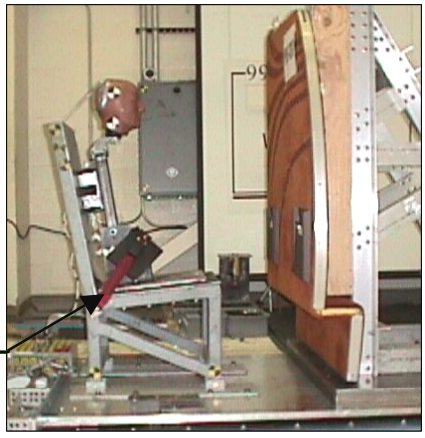

FIGURE 9. PHCT MODEL

FIGURE 10. PHCT SETUP ON SLED

The PHCT was placed at a seat setback distance of 35 inches. The seat and the bulkhead were positioned to achieve the seat setback distance. A lap belt was used to restrain the PHCT. A load cell was attached to the left lap belt to measured belt loads. Head c.g. acceleration data was obtained from a triaxial accelerometer mounted in the head. Two video-tracking targets were mounted on the upper and lower portion of the head to obtain the head impact angle and velocity. A video-tracking target was also mounted on the pendulum base. A PHCT test was performed under the same conditions as FSST 99137-02. Figure 11 shows the full-scale sled pretest setup and posttest condition.

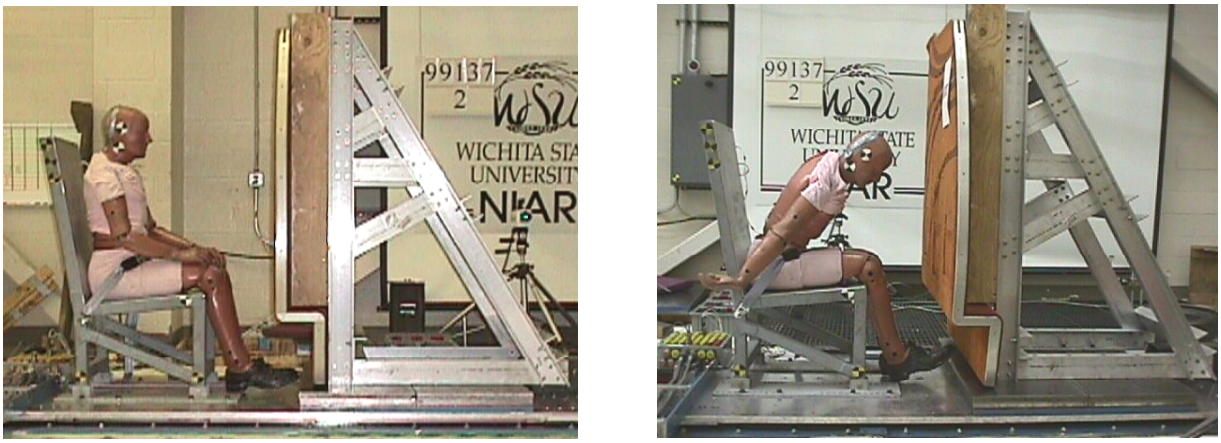

(a) Pretest (b) Posttest

FIGURE 11. FSST 99137-02 (a) PRETEST AND (b) POSTTEST

A summary of the PHCT and FSST test results are shown in table 1. The kinematics of the PHCT and FSST tests are shown in figure 12 and are comparable. The maximum translation of the PHCT and FSST tests showed similar amounts of translation of the pelvis (about 6 inches). Table 1 shows that the head peak resultant accelerations, the head average resultant accelerations, and HIC values for the two tests were not similar. The PHCT had a higher head impact velocity and lower head impact angle than the FSST. The data summary sheets for the PHCT and FSST are given in appendix B.

TABLE 1. COMPARISON OF PHCT AND FSST TEST RESULTS

Results	PHCT Test 99109-02	FSST Test 99137-02
Head impact angle (deg)	39	48
Head impact velocity (ft/sec)	46	42
Sled peak acceleration (g's)	17.3	16.4
HIC	646	1020
HIC window (ms)	21.4	19.6
Head c.g. peak resultant acceleration (g's)	77	106
Head c.g. average resultant acceleration (g's)	62	77

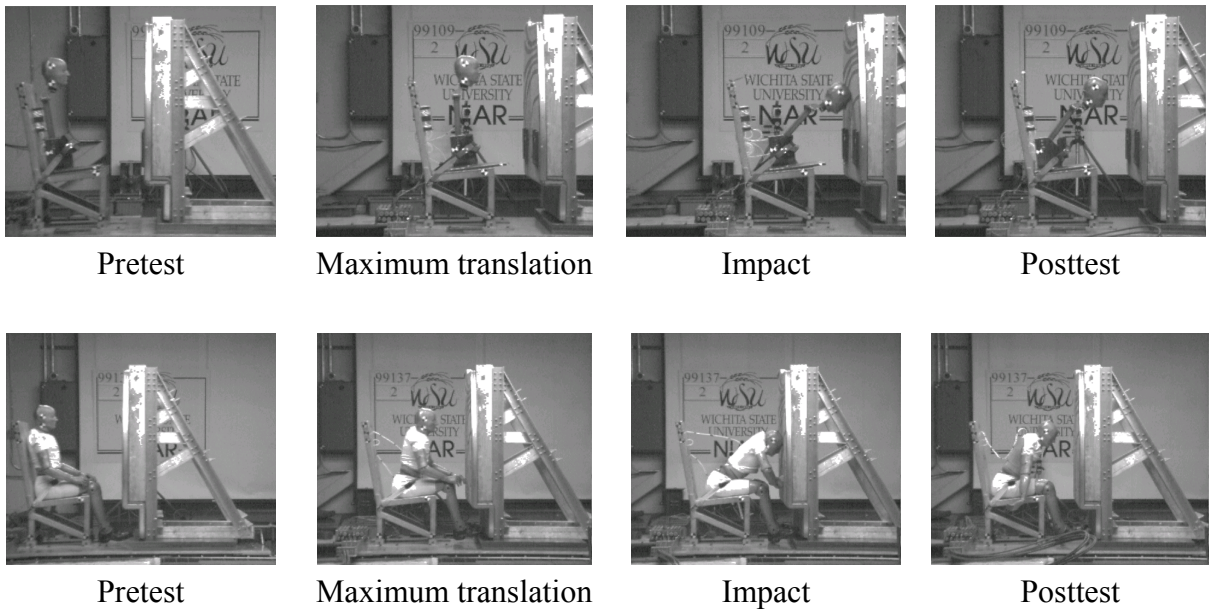

FIGURE 12. COMPARISON OF KINEMATICS OF PHCT AND FSST

The head c.g. resultant acceleration comparison of the two tests is shown in figure 13. The head c.g. resultant acceleration profile of the PHCT and FSST tests shows reasonable agreement. The HIC window obtained for both the tests is similar.

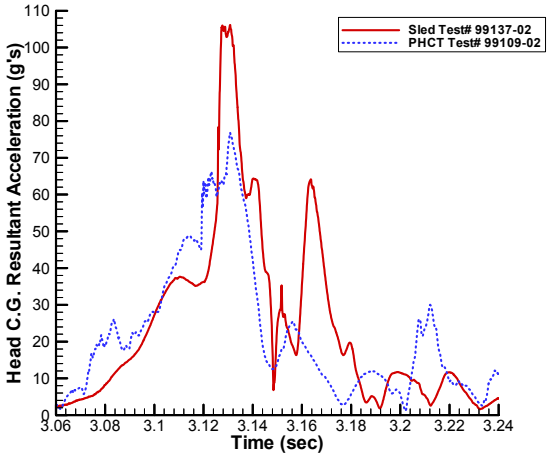

FIGURE 13. HEAD c.g. RESULTANT ACCELERATION COMPARISON OF PHCT SLED TEST WITH FSST

Based on results obtained from the PHCT test, parametric studies using mathematical analysis were conducted on the PHCT model to obtain a final weight and weight distribution, see figure 14. This weight distribution best represented the kinematics of the PHCT model with the FSST. The reason for this difference is to compensate for the effects of varying inertia associated with articulating ATD arms and legs during a dynamic test.

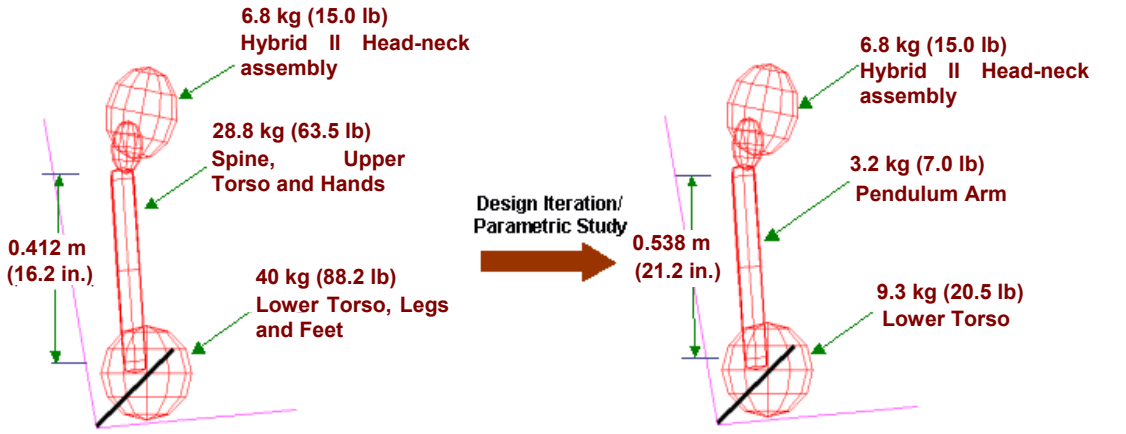

FIGURE 14. FINAL WEIGHT DISTRIBUTION OF THE PHCT MODEL

3.3 DEVELOPMENT OF HIC COMPONENT TESTER (HCT) (STEPS D, E, AND F IN FIGURE 1).

Using the information obtained in steps A-C of figure 1, the HCT was designed, analytically modeled, refined, and fabricated. The HCT (figures 15 and 16) consists of a Hybrid II ATD head mounted to an aluminum (Al) pendulum arm (collectively the upper torso) attached to a translating aluminum mass representing the lower torso. The pendulum arm weighs 7 lbs and is 21.2 inches long and is pinned to the lower torso, allowing the pendulum to pivot. The lower torso is hollow with the provision for adding mass in the event it is necessary to fine-tune the system. The Hybrid II ATD head is connected to the pendulum arm through the neck bracket. The flexible neck of the Hybrid II ATD was found to break often when used in the component test. This was due to the rigid pendulum arm that caused high bulkhead impact forces to be transmitted to the neck. The flexible neck was, therefore, replaced with a rigid polycarbonate neck. An actuator provides angular motion to the pendulum through a pivoting support arm and the attached support arm extension. The actuator is mounted on a stand and is supported by bearings on either end of the trunion. The stand assembly and support arm are bolted in place. The lower torso is attached to two sets of linear bearings that slide on the rails, allowing it to translate forward and aft. This translation represents the ATD snap back in an FSST. Finite element analysis tools were used to evaluate the performance of critical components such as the support arm extension, pendulum arm, stand, and the actuator plate. The detailed engineering drawings of individual components of the system are given in appendix C.

Head c.g. acceleration data is obtained from a triaxial accelerometer mounted in the head. The data is recorded using a high-speed data acquisition system (sampled at 10 kHz) and filtered using an SAE J211Class 1000 filter (1667 Hz). Two video-tracking targets were mounted on the upper and lower portion of the head. The test was recorded using a high-speed video recording system (1000 frames per second). The head impact angle, velocity, and location were determined from the video of the test.

The propulsion system consists of a bottle of pressurized nitrogen gas, an accumulator, a gas shutoff valve, tubing, and a control system. Pressurized nitrogen gas is used to charge the accumulator to the required pressure. The accumulator, when triggered by the control system, discharges the nitrogen gas instantaneously through the actuator providing angular velocity to the pendulum arm. The propulsion system and control system components are discussed in detail in appendix D.

The analytical model and assembly of the HCT are shown in figures 15 and 16, respectively.

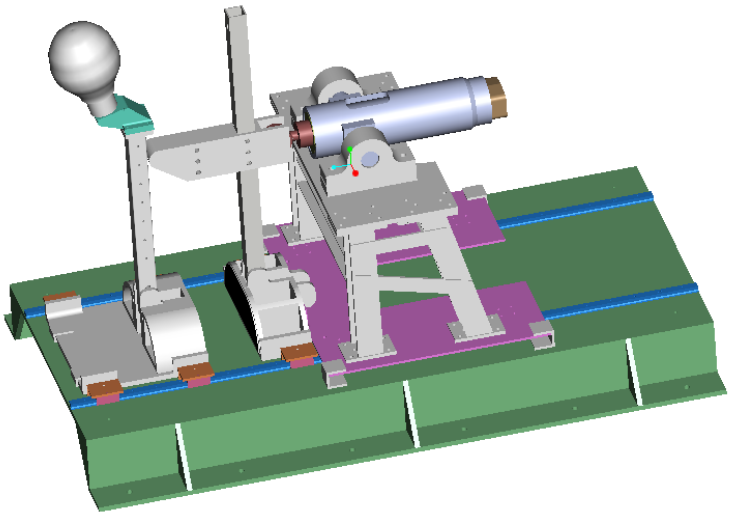

FIGURE 15. ANALYTICAL MODEL OF HCT

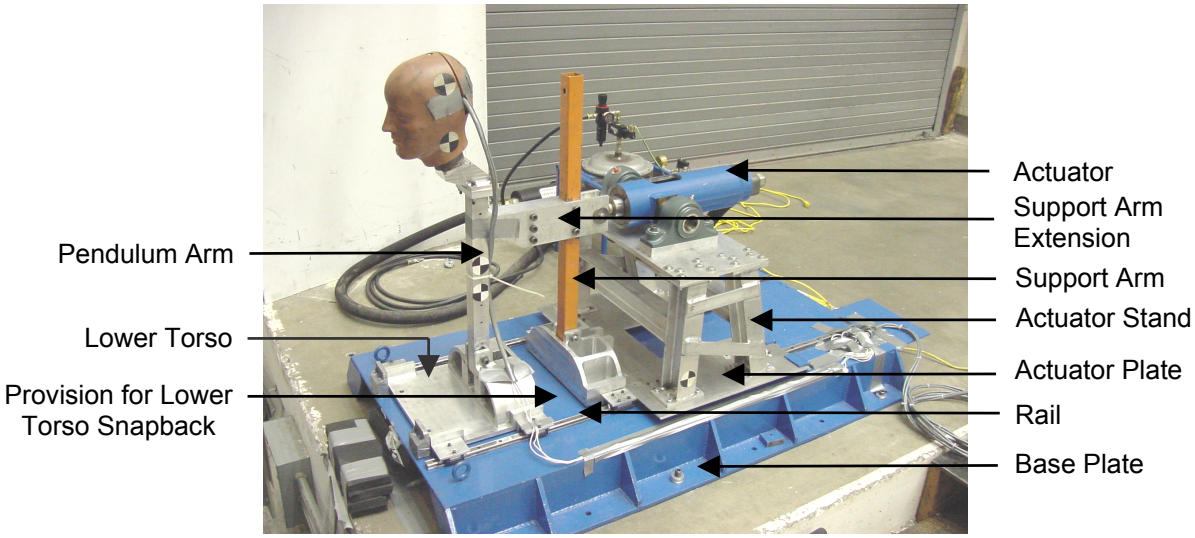

FIGURE 16. ASSEMBLY OF THE HCT

The HCT can be operated in two modes. Figure 17 shows the Mode I and Mode II configurations. In Mode I, the lower torso is rigidly fixed to the base plate and the actuator is operated to rotate the pendulum arm thus providing only one degree of freedom. In Mode II, the

lower torso is free to translate on linear bearings providing a second degree of freedom. This provision for the lower torso to snap back at the time of head impact is provided to mimic the ATD snapback in an FSST.

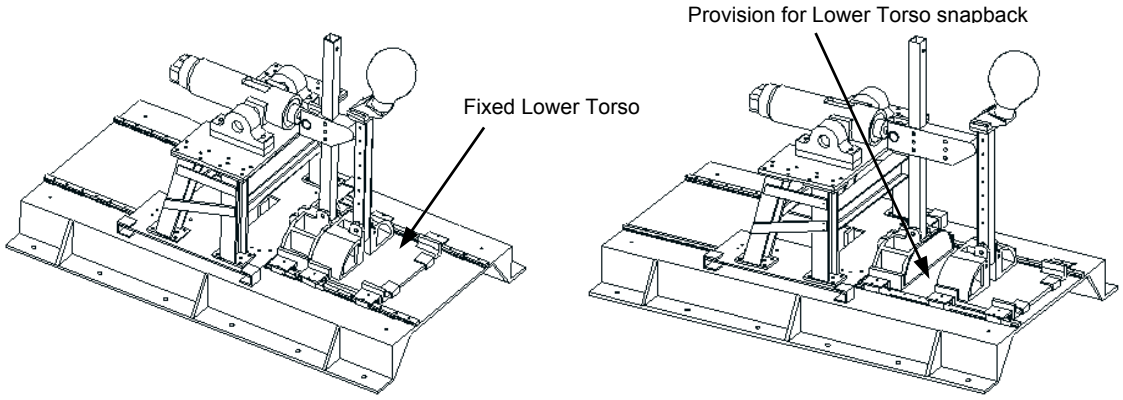

Mode I Configuration Mode II Configuration

FIGURE 17. HCT MODE I AND MODE II CONFIGURATIONS

3.4 OPERATING METHODOLOGY/SYSTEM CALIBRATION (STEP G IN FIGURE 1).

The operating methodology for calibrating the component HIC tester is shown in figure 18, and the corresponding flow chart shown in figure 19.

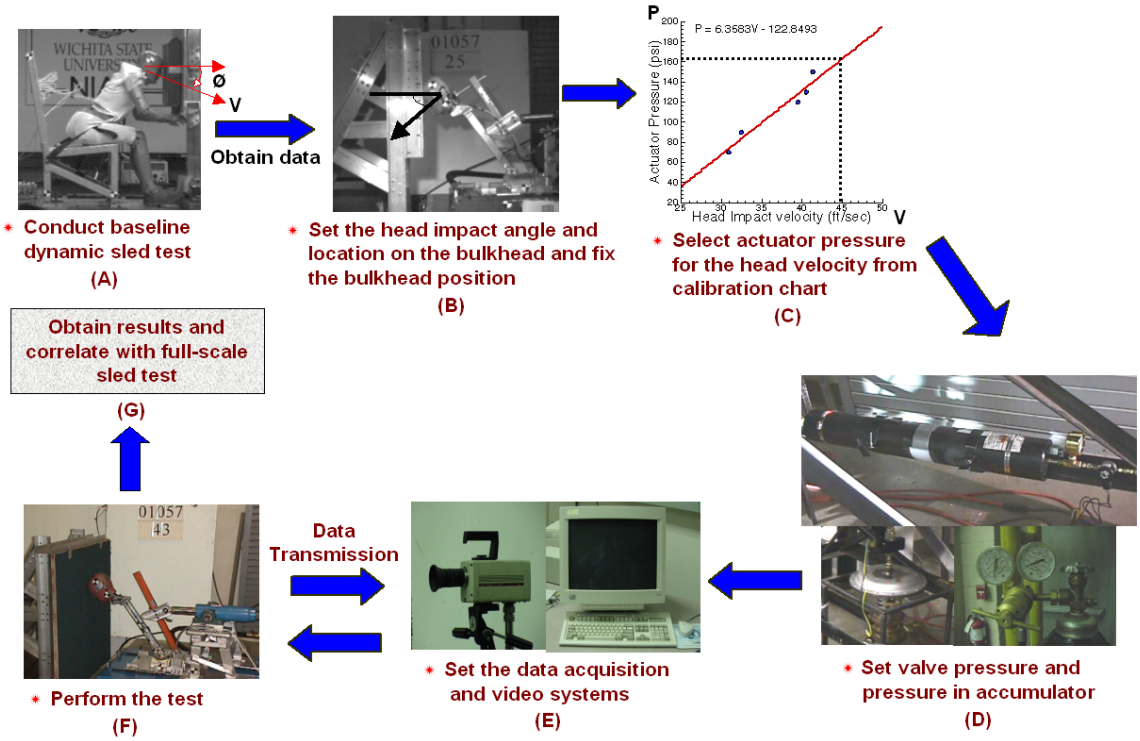

FIGURE 18. OPERATING METHODOLOGY FOR HCT

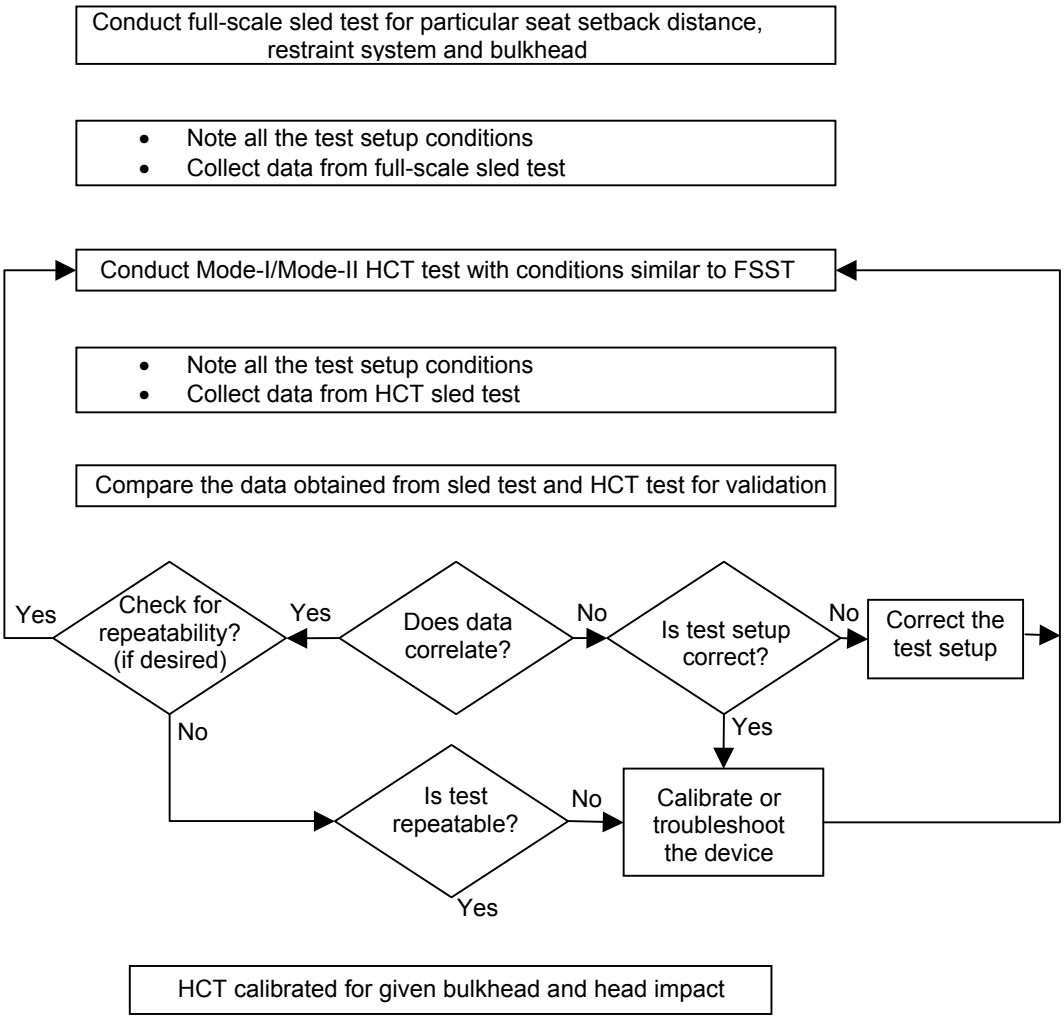

FIGURE 19. FLOW CHART FOR OPERATING/CALIBRATING THE HCT

A baseline FSST is conducted to obtain the head impact angle and velocity. The HCT is configured for Mode I or Mode II operation by selecting the appropriate support arm extension. The lower torso is secured to the base plate for Mode I operation or allowed to translate for Mode II operation. In both modes, the pendulum arm is perpendicular to the base plate and is in contact with the support arm extension. The bulkhead is moved forward and aft to achieve the required head impact angle and fixed in this position. A pressure-velocity calibration chart is used to obtain the actuator pressure to achieve the required head impact velocity. The data acquisition and video systems are initialized and set to record the head acceleration data and videotape the test. A HCT test is performed, if the results are comparable to the FSST, the system is calibrated, and additional component tests may be conducted. If the results are not comparable, the system is diagnosed to determine the problem. A detailed procedure for obtaining the pressure-velocity calibration charts from the calibration tests is given in appendix E.

3.5 EVALUATION OF HCT USING AN ALUMINUM BULKHEAD.

Several tests were conducted with the HCT using the same setup configuration as in FSST 96288-004. A bulkhead consisting of Al 2024-T3, 0.063 in. thick, was used. The objective of these tests was to compare the data obtained from the HCT with that of the FSST. Tests in both Mode I and Mode II were conducted. The setup for the FSST and sequence of motion is shown in figures 20 and 21, respectively. The data summary sheet for the FSST is given in appendix B.

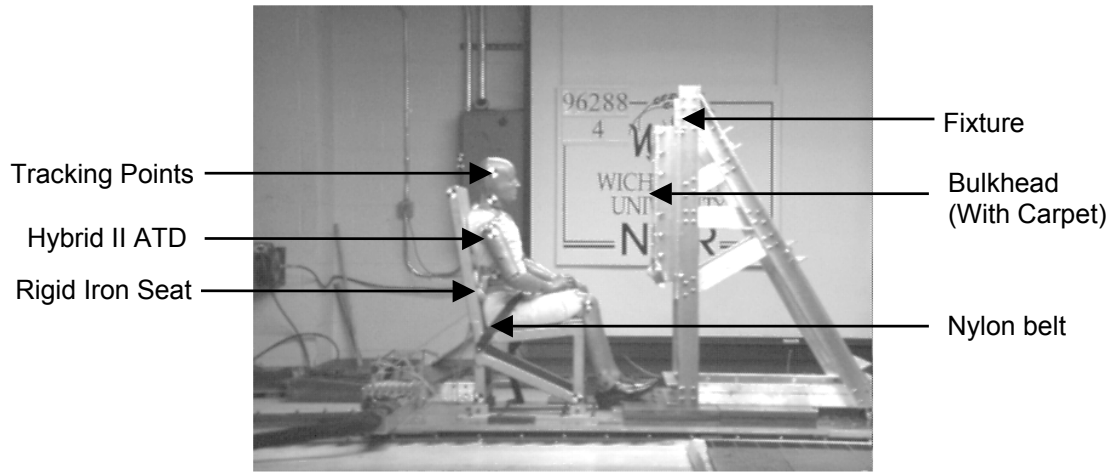

FIGURE 20. SETUP FOR ALUMINUM BULKHEAD SLED TEST

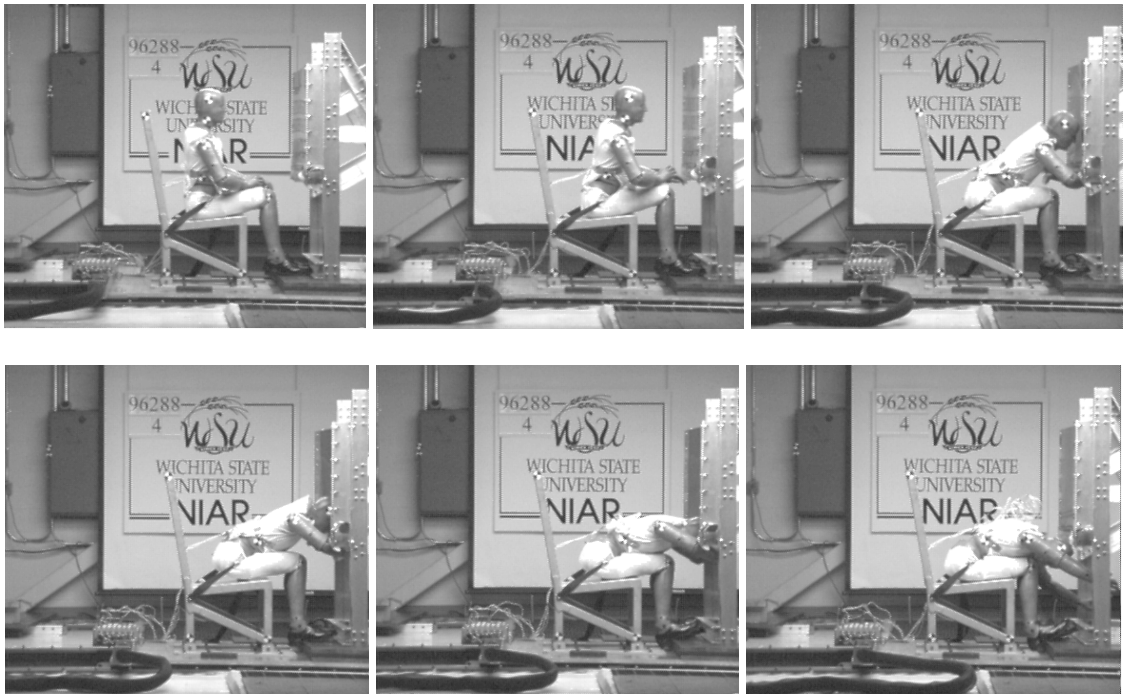

FIGURE 21. SEQUENCE OF MOTION OF SLED TEST 96288-004

3.5.1 Mode I.

Tests 01057-24 and -25 were conducted in Mode I and the data compared with FSST 96288-004. Figure 22 shows the sequence of motion for the HCT during test 01057-25. The data summary sheets for individual component tests are given in appendix F.

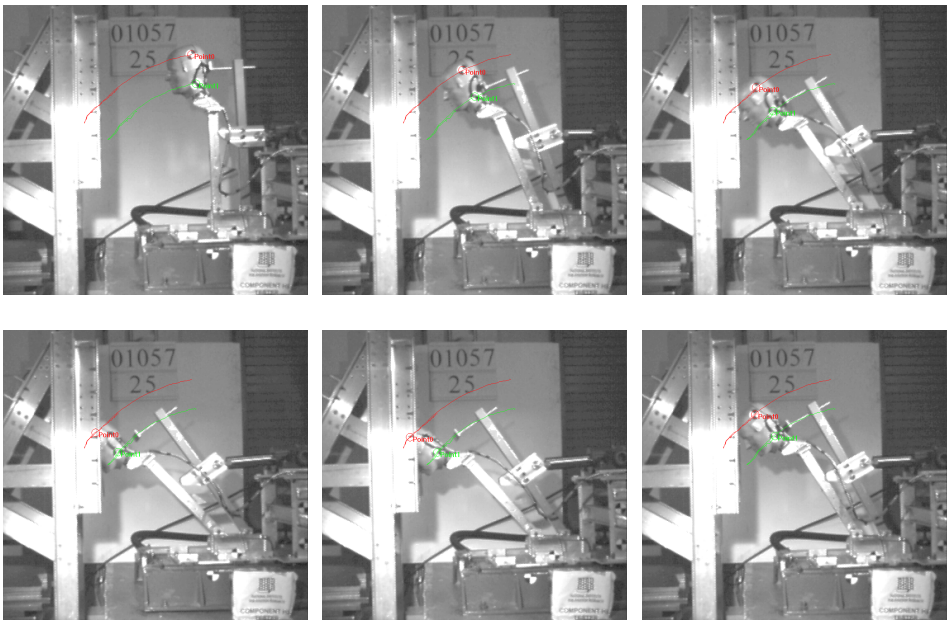

FIGURE 22. SEQUENCE OF MOTION OF HCT DURING TEST 01057-25

The results are summarized in table 2. It is observed that the HIC, HIC window, peak, and average head c.g. resultant accelerations show good agreement.

TABLE 2. COMPARISON OF HCT TESTS AND FSST IN MODE I (ALUMINUM BULKHEAD)

Parameter	FSST 96288-004	HCT Test 01057-24	HCT Test 01057-25
Head impact angle (deg.)	38	37	38
Head impact velocity (ft/sec)	45	41	44
HIC	694	763	706
HIC window (ms)	23.7	20.8	21.8
Head c.g. peak resultant acceleration (g's)	143	145	143
Head c.g. average resultant acceleration (g's)	61	67	64

Comparison plots of the HCT tests and the FSST are shown in figure 23. The resultant head c.g. acceleration profiles show poor correlation.

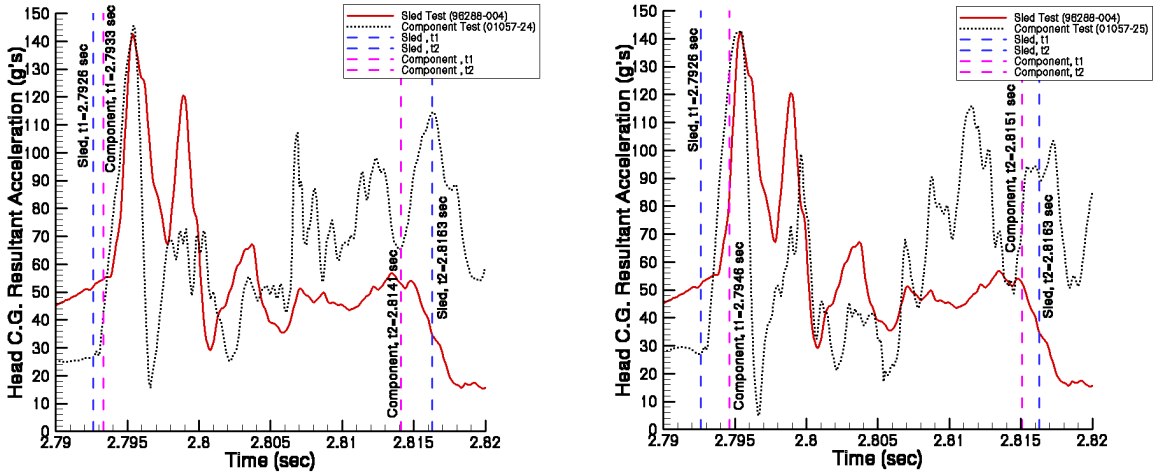

FIGURE 23. COMPARISION PLOTS OF HCT TESTS 01057-24 AND -25 AND FSST 96288-004

The HCT was checked for repeatability using two consecutive tests with identical setup configurations. From the HCT tests conducted in Mode I, it was found that the tester shows repeatability, as shown in figure 24.

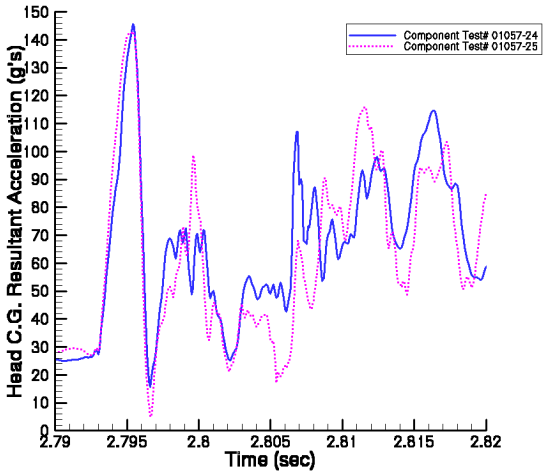

FIGURE 24. REPEATABILITY OF HCT TESTS 01057-24 AND -25

3.5.2 Mode II.

Tests 01057-27, -28, and -29 were conducted in Mode II and the data compared with FSST 96288-004. Figure 25 shows the sequence of motion for the HCT during test 01057-27. The data summary sheets for individual tests are given in appendix F.

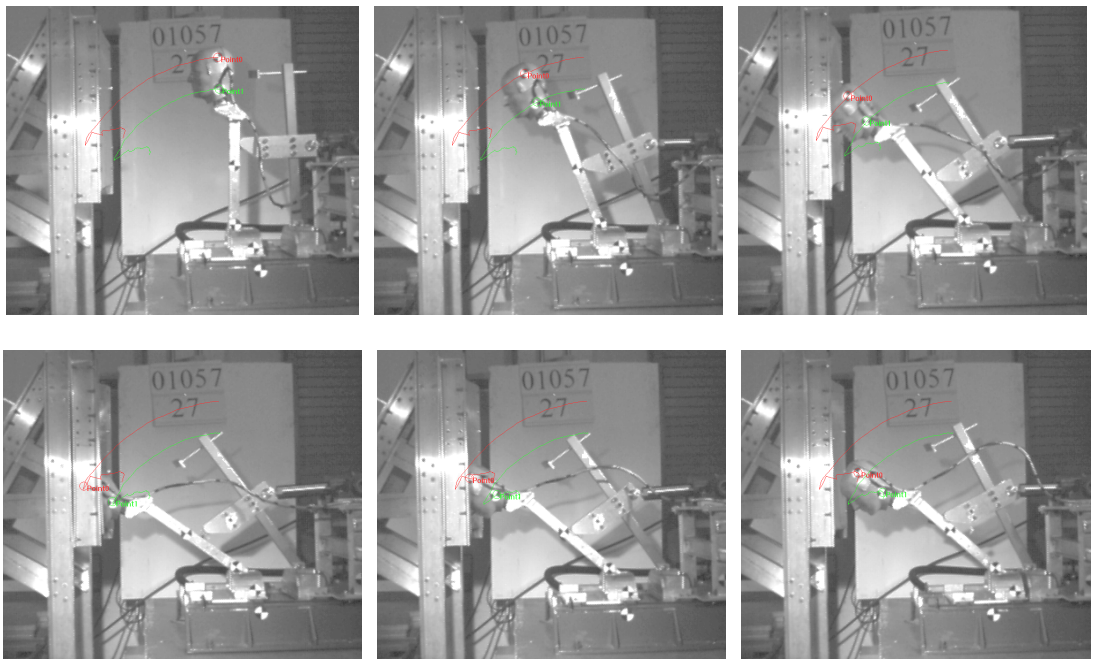

FIGURE 25. SEQUENCE OF MOTION OF HCT DURING TEST 01057-27

The results are summarized in table 3. It is observed that the HIC, HIC window, peak, and average head c.g. resultant accelerations show good agreement.

TABLE 3. COMPARISON OF HCT TESTS AND FSST IN MODE II (ALUMINUM BULKHEAD)

Description	FSST 96288-04	HCT Test 01057-27	HCT Test 01057-28	HCT Test 01057-29
Head impact angle (deg)	38	37	39	36
Head impact velocity (ft/sec)	45	45	40	46
HIC	694	746	752	729
HIC window (ms)	23.7	22.9	24.8	23.9
Head c.g. peak resultant Acceleration (g's)	143	141	136	139
Head c.g. average resultant acceleration (g's)	61	64	62	62

Comparison plots of the HCT tests with the FSST are shown in figure 26. The resultant head c.g. acceleration profiles show poor correlation.

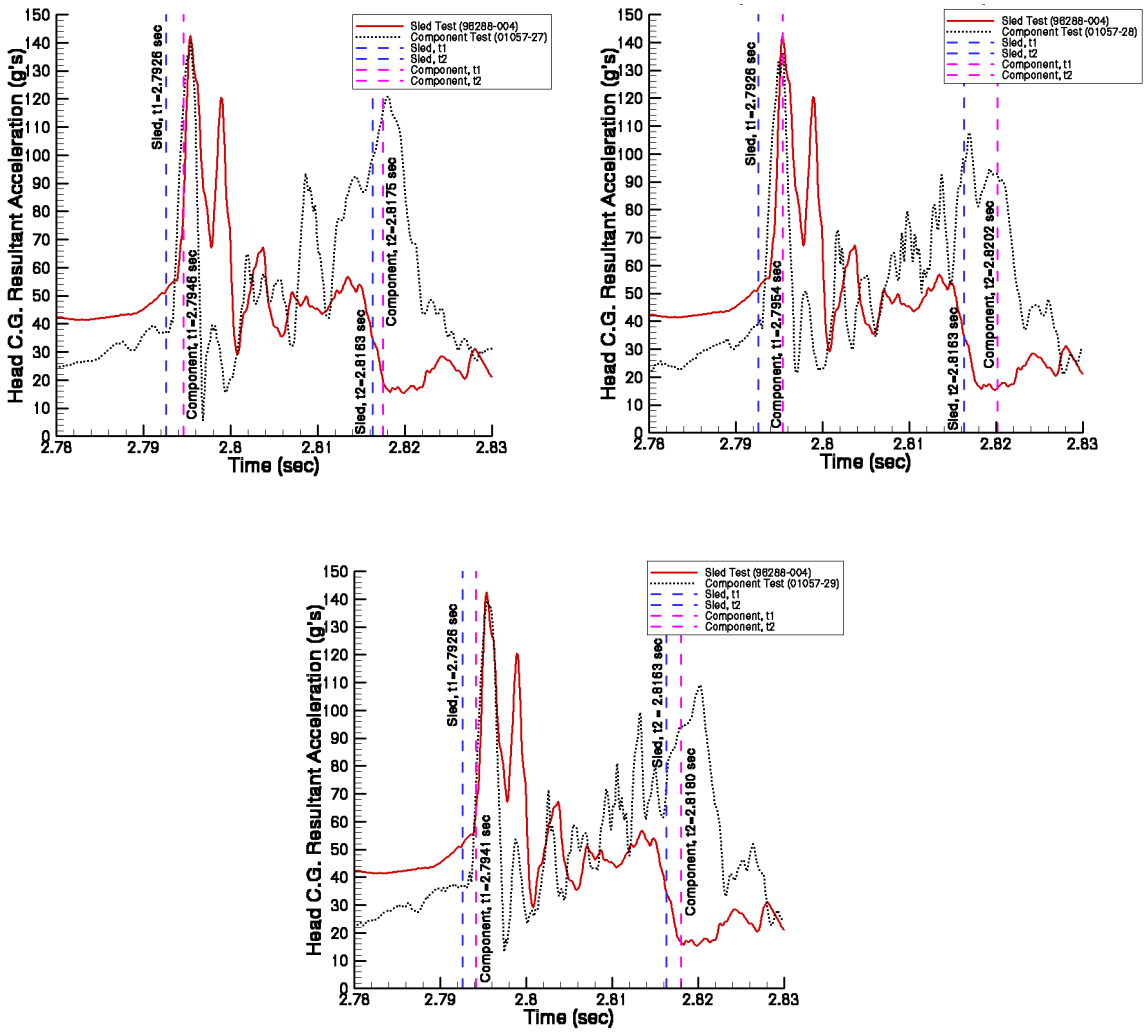

FIGURE 26. COMPARISON PLOTS OF HCT TESTS 01057-27, -28, AND -29 AND FSST 96288-004

The HCT was checked for repeatability using two consecutive tests with identical setup configurations. From the HCT tests conducted in Mode II, it was found that the tester showed repeatability, as shown in the figure 27.

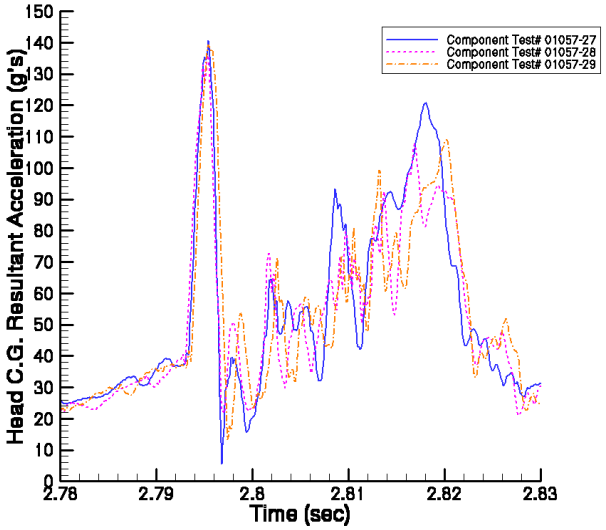

FIGURE 27. REPEATABILITY OF HCT TESTS 01057-27, -28, AND -29

3.6 EVALUATION OF HCT USING A NOMEX HONEYCOMB BULKHEAD.

Results from FSST 01008-8 were used as a comparison for HCT tests conducted using a 1″ thick Nomex honeycomb panel. The HCT had the same configuration as the FSST. Tests in both Mode I and Mode II configuration were conducted. The setup for the FSST and sequence of motion is shown in figures 28 and 29, respectively. The data summary sheet for the FSST is given in appendix B.

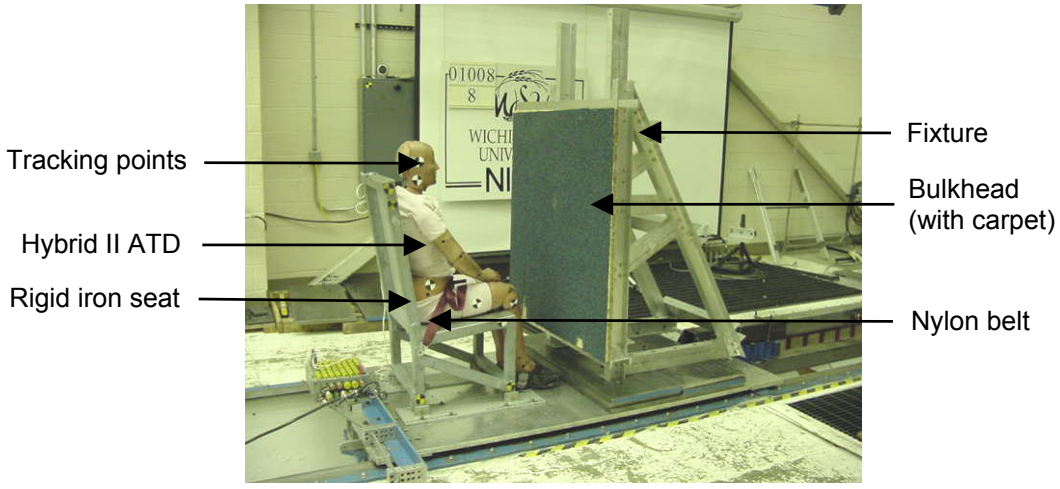

FIGURE 28. SETUP FOR NOMEX HONEYCOMB BULKHEAD SLED TEST

FIGURE 29. SEQUENCE OF MOTION OF SLED TEST 01008-8

3.6.1 Mode I.

HCT tests 01057-43 and -44 were conducted in Mode I and the data compared with FSST 01008-8. Figure 30 shows the sequence of motion for the HCT during test 01057-43. Data summary sheets for the above component tests are given in appendix F.

FIGURE 30. SEQUENCE OF MOTION OF HCT DURING TEST 01057-43

The results are summarized in table 4. It is observed that there is little agreement between the HCT and the FSST HIC parameters. The head impact angles, head impact velocities, and HIC windows were low, while the head c.g. average resultant acceleration was high. Only the head c.g. peak resultant acceleration was similar consistently.

TABLE 4. COMPARISON OF HCT TESTS AND FSST IN MODE I (HONEYCOMB BULKHEAD)

Parameter	FSST 01008-8	HCT Test 01057-43	HCT Test 01057-44
Head impact angle (deg)	40	37	38
Head impact velocity (ft/sec)	45	40	40
HIC	783	834	981
HIC window (ms)	44.4	32.9	31.8
Head c.g. peak resultant acceleration (g's)	132	130	*136
Head c.g. average resultant acceleration (g's)	50	58	63

*Value of initial significant peak.

Comparison of the HCT tests with the FSST is shown in figure 31. The head c.g. resultant acceleration profiles show poor correlation.

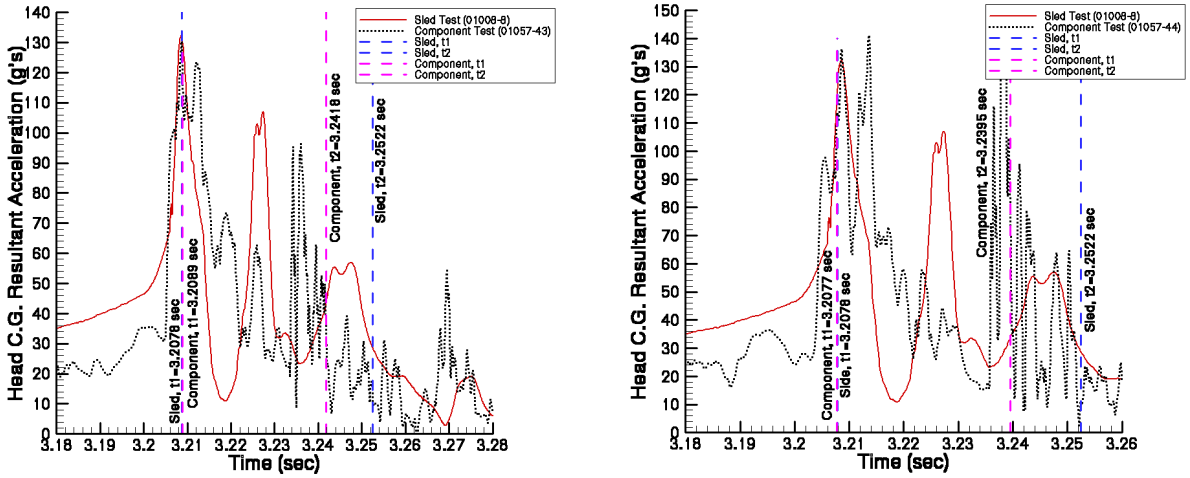

FIGURE 31. COMPARISON PLOTS OF HCT TESTS 01057-43 AND -44 AND FSST 01008-8

The HCT was checked for repeatability using two consecutive tests with identical setup configurations. From the HCT tests conducted in Mode I, it was found that the tester showed repeatability, as shown in figure 32.

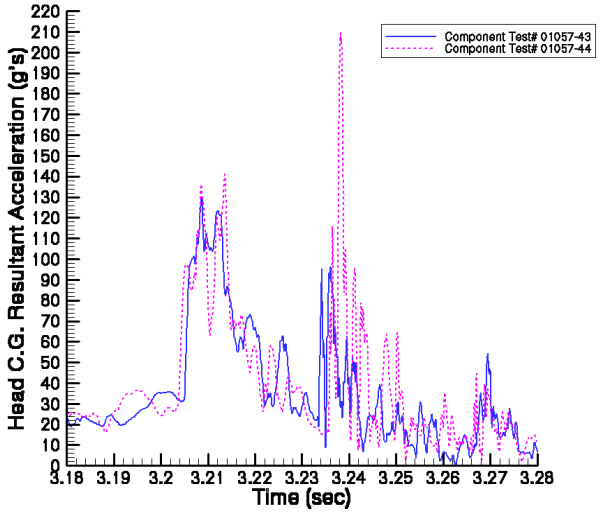

FIGURE 32. REPEATABILITY OF HCT TESTS 01057-43 AND -44

3.6.2 Mode II.

HCT test 01057-49 was conducted in Mode II and the data compared with FSST 01008-8. The test was conducted using a honeycomb bulkhead. Figure 33 shows the test sequence of the HCT during test 01057-49. A data summary sheet for the above component test is given in appendix F.

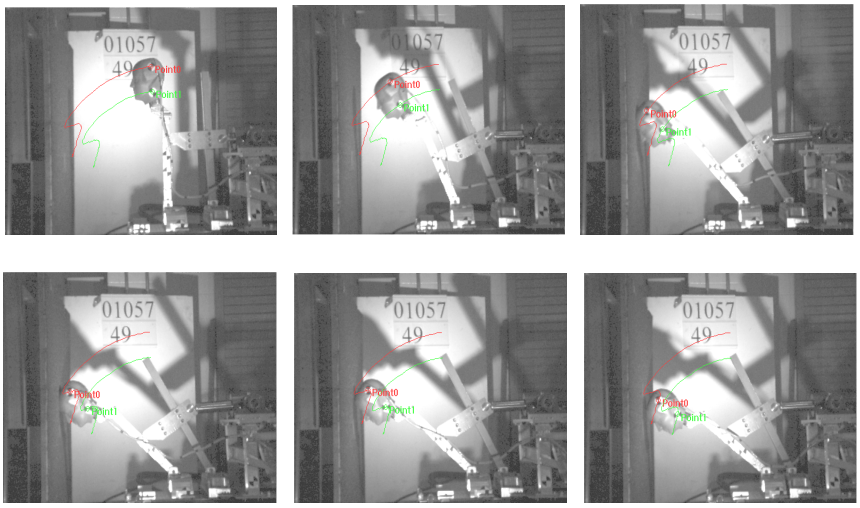

FIGURE 33. SEQUENCE OF MOTION OF HCT DURING TEST 01057-49

The results are summarized in table 5. It is observed that there is little agreement between the HCT and the FSST HIC parameters. The head impact velocity, head c.g. peak resultant acceleration, and HIC window were low, while the HIC and head c.g. average resultant acceleration were high.

TABLE 5. COMPARISON OF HCT TESTS AND FSST IN MODE II (HONEYCOMB BULKHEAD)

Parameter	FSST 01008-8	HCT Test 01057-49
Head impact angle (deg)	40	39
Head impact velocity (ft/sec)	45	41
HIC	783	960
HIC window (ms)	44.4	31.8
Head c.g. peak resultant acceleration (g's)	132	109
Head c.g. average resultant acceleration (g's)	50	62

Comparison of the HCT tests with the FSST is shown in figure 34. The resultant acceleration profiles show poor correlation.

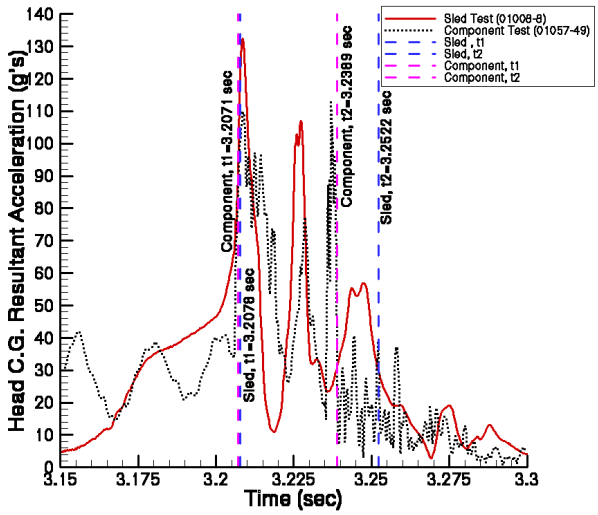

FIGURE 34. COMPARISON PLOTS OF HCT TEST 01057-49 AND FSST 01008-8

The HCT was not tested for repeatability in Mode II.

4. MODE I VS MODE II.

Comparisons of Mode I and Mode II data for the aluminum bulkhead and Nomex honeycomb bulkheads show no difference between the modes. There was little agreement between the HCT and the FSST for the Nomex honeycomb bulkhead. However, there was not sufficient data for a conclusive determination.

5. OPERATIONAL ANALYSIS OF HCT.

A system review was undertaken to determine if improvements could be made to the HCT and its operation. The most significant issues were:

- Tendency for the upper torso (pendulum arm) to contact the support arm assembly during rebound. This contact influenced the measured accelerations and associated HIC parameters.

- Operating pressures improperly set.

- Effect of adding mass to the lower torso not evaluated.

- Improved calibration curve for operating pressure versus required head impact velocity (greater range).

- No determination of appropriate mode of operation.

6. CONCLUSIONS.

The HIC component tester (HCT) was designed and fabricated as an alternate method to determine the head injury criteria (HIC) value for aircraft seat certification. The HCT could be used to evaluate different designs and test conditions at a reduced cost and in a shorter time than full-scale sled tests. The HCT has two modes of operation. Mode I uses a fixed base while Mode II uses a translating base to emulate some of the biodynamic characteristics associated with an anthropomorphic test dummy (ATD) in a full-scale sled test. Preliminary results from the HCT have been compared with results from full-scale sled tests. Comparisons were based on the head impact angle, head impact velocity, HIC, HIC window, peak head center of gravity (c.g.) resultant acceleration, average head c.g. resultant acceleration, and head c.g. resultant acceleration profiles. The comparisons were made for both modes of operation using aluminum type bulkheads and Nomex honeycomb type bulkheads.

For the aluminum type bulkhead, the HIC, HIC window, and peak average head c.g. resultant acceleration showed good agreement. However, the head c.g. resultant acceleration profiles did not. The HCT showed repeatability for both modes. The results for both modes of operation were similar.

For the Nomex honeycomb type bulkhead, the HIC, HIC window, and peak average head c.g. resultant acceleration showed little agreement. The resultant acceleration profiles show poor agreement. The HCT showed repeatability for Mode I. A repeatability test was not conducted for Mode II. The results for both modes of operation were similar.

Comparisons of Mode I and Mode II data for the aluminum bulkhead and Nomex honeycomb bulkheads show no difference between the modes. There was little agreement between the HCT and the FSST for the Nomex honeycomb bulkhead. There was not sufficient data for a conclusive determination.

7. REFERENCES.

1. Chandler, R.F., "Human Injury Criteria Relative to Civil Aircraft Seat and Restraint Systems," SAE Paper 851847, Society of Automotive Engineers, Warrendale, PA, 1985.

2. Lissner, H.R., Lebow, M., and Evans, F.G., "Experimental Studies on the Relation Between Acceleration and Intracranial Pressure Changes in Man," Surgery, Gynecology, and Obstetrics, V. 111, pp. 329-338, 1960.

3. Gadd, C.W., "Use of a Weighted Impulse Criterion for Estimating Injury Hazard," SAE Paper 660793, *Proceedings of the Tenth Stapp Car Crash Conference*, pp. 16-174, Society of Automotive Engineers, Warrendale, Pennsylvania, 1966.

4. Versace, J., "A Review of the Severity Index," SAE Paper 710881, *Proceedings of the Fifteenth Stapp Car Crash Conference*, pp. 771-796, Society of Automotive Engineers, Warrendale, Pennsylvania, 1971.

5. Gurdjian, E.S., Lissner, H.R., Latimer, F.R., Haddad, B.f., and Webster, J.E., "Quantitative Determination of Acceleration and Intercranial Pressure in Experimental Head Injury," Neurology 3,4 4223, 1953.

6. Gurdjian, E.S., Roberts, V.L., and Thomas, L.M., "Tolerance Curves of Acceleration and Intercranial Pressure and Protective Index in Experimental Head Injury," *J. of Trauma*, Vol. 6, pp. 600, 1964.

7. Department of Transportation (1971) Occupant Crash Protection – Head Injury Criterion, NHTSA Doc Number 69-7, Notice 19, S6.2 of FMVSS 208, March 1971.

8. Title 14 Code of Federal Regulations, Part 23, Amendment 23-39, Section 23.562, published in the Federal Register, August 14, 1988.

9. Title 14 Code of Federal Regulations, Part 25, Amendment 25-64, Section 25.562, published in the Federal Register, May 17, 1988.

10. Lankarani, H.M, Hooper, S.J, and Mirza, M.C, "An Evaluation of a Component HIC Apparatus," National Institute for Aviation Research, Wichita State University, August 1998.

11. Hooper, S.J., Lankarani, H.M., and Mirza, M.C., "Parametric Study of Crashworthy Bulkhead Designs," FAA William J. Hughes Technical Center, NJ, in publication process.

12. MADYMO V5.4, TNO Automotive, May 1999.

APPENDIX A—EXISTING COMPONENT LEVEL DEVICE

A.1 BOWLING BALL TESTER.

The instrumented ball impact test procedure was one of the means to evaluate HIC for head impact onto aircraft interior structures. This procedure was selected based on a technical paper presented by the Federal Aviation Administration Civil Aeromedical Institute (FAA CAMI) [A-1], which specifies three basic options for complying with requirements for head impact protection for seat installations located aft of cabin structures. The Biodynamic Research Station of FAA CAMI conducted a bowling ball drop test, in which an instrumented bowling ball was made to impact various padding materials and the results were compared with that obtained from sled tests. A procedure for the instrumented ball impacts was defined in Advisory Circular (AC) 25-17. The experimental setup for the bowling ball test is shown in figure A-1.

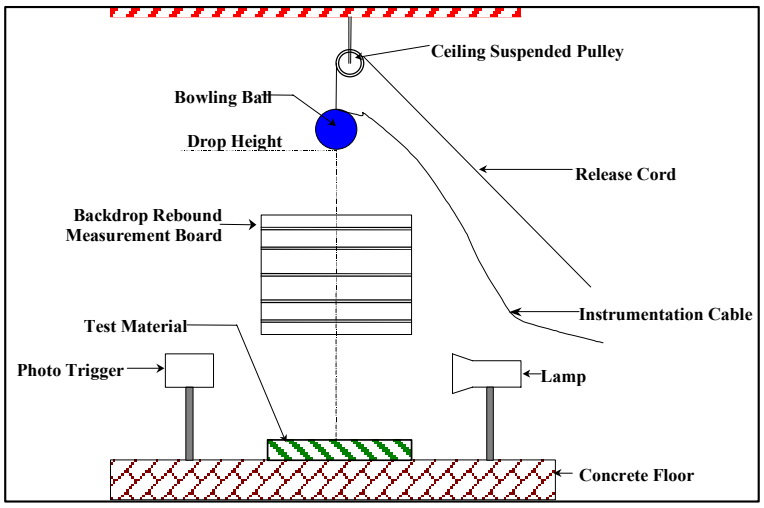

FIGURE A-1. BOWLING BALL TEST SETUP

Tests were conducted by raising the ball to the desired height through a pulley suspended from a ceiling beam. The ball drops freely onto the test material from manual release at the free end of the cord. An infrared photo sensor in the path of the falling ball generates the electronic signal to trigger the data acquisition system before impact. The rebound kinetic energy was derived from the maximum rebound height, which was measured directly from the high-speed video data collected from the test.

Some of the drawbacks of this tester are (1) it does not account for the kinematics of moving body parts, (2) it only permits a normal impact into the surface (not impact location sensitive), and (3) does not account for facial features.

A.2 FREE MOTION HEADFORM TESTER.

The free motion headform (FMH) tester was designed to permit the simulation of head impacts common in the automotive crash environment [A-2]. However, it is only used by the automotive industry for impact tests on rigid surfaces to supplement full-scale impact tests. The device is

not used on aircraft because it was only validated for a head impact velocity of only 15 ft/sec, which is about 1/3 of typical aircraft head strike velocities. The main objective was to develop a head component design that represented the impact of an actual head. In a head component test, there is much greater control of the head impact location, and the tests are less expensive than a full-scale sled test.

Figure A-2 shows the typical setup of a FMH tester, which was used in the automotive industry to test a variety of surfaces. A featureless Hybrid III headform was developed to assess the interior impact behavior of an occupant in a vehicle collision. It is basically a standard Hybrid III head without a nose.

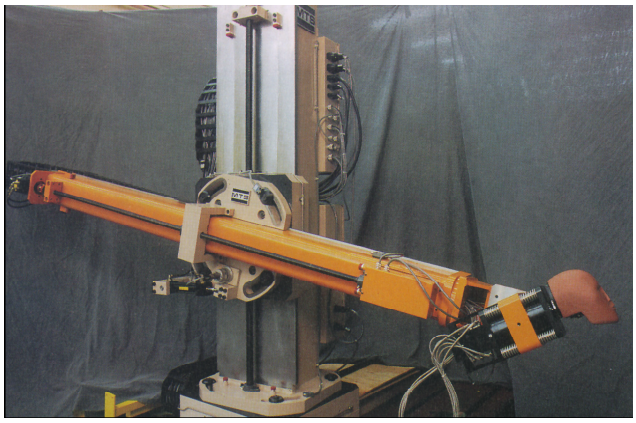

FIGURE A-2. FREE MOTION HEADFORM TESTER

The back of the head, i.e., the skullcap, was removed and replaced by a plate for mounting to a propulsion shaft. It consists of a hollow cast aluminum shell covered with a layer of vinyl rubber. The Hybrid III headform was mounted on a compressible fluid impact accelerator and held against the impactor ram by a permanent magnet. When the impactor was fired, the ram separated the headform from the permanent magnet. During the ram acceleration, the headform was held against the ram by its inertial force. Upon deceleration, the headform separated and impacted the test surface in free flight.

The main advantage of the FMH tester was its ability to impact surfaces without the requirement of being normal to the impacting surface. This allowed components to be tested in a more realistic manner. The drawbacks of this system were the higher head injury criteria (HIC) values and peak head accelerations, compared to a full-scale sled model. This was due to the entire energy being transferred directly to the head, which in turn was absorbed by the bulkhead. In the FMH tester, the headform completely interacts with the bulkhead panel, while in the sled test, there are interactions among various body parts and belt restraining system on the lower torso that affected the results.

A.3 MGA HEAD/NECK IMPACTOR.

The MGA head/neck impactor is shown in figure A-3. This test device is an inverted pendulum type impactor and consists of an accelerator, pendulum arm, support arm, rebound brake system,

anthropomorphic test dummy (ATD) head/neck assembly, signal conditioning system, and data acquisition system operated via computerized control. The two parameters required to simulate a representative sled test are head impact velocity and impact angle.

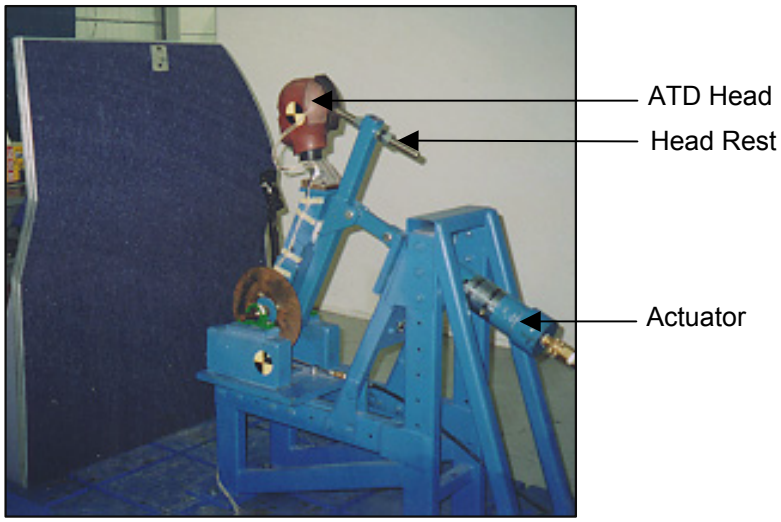

FIGURE A-3. MGA HEAD/NECK IMPACTOR

The device consists of a 49 Code of Federal Regulations Part 572 head and neck assembly mounted to a pivoting arm and accelerated by a pneumatic actuator. The head accelerations were measured using a triaxial accelerometer mounted in the head. A velocity trap was used to measure the arm velocity just prior to impact. Video data was acquired using high-speed cameras. The desired head impact angle was achieved by changing the test panel distance from the impactor. Once the head impact angle was adjusted, the panel was fixed in position. The head impact velocity was achieved by adjusting the nitrogen gas pressure in the actuator.

The device has been evaluated as a part of an investigation addressing the front-row HIC problem [A-3]. This study has shown the MGA tester to be very effective for shorter setback distances and bulkhead with hard impact surfaces.

A.4 PENDULUM RIG TESTER.

The pendulum rig tester is shown in figure A-4. The pendulum test rig was developed at the National Institute for Aviation Research at Wichita State University and is capable of simulating the impact of an occupant onto the interior structure or the impact on a pedestrian. The pendulum is 19 feet in length and is capable of achieving velocities above 50 ft/sec at impact. The pendulum method is a cost-effective method for finding the various injury criteria in head impact collisions and is similar to the FMH and bowling ball tests. The pendulum test rig consists of a main striking pendulum, which is brought to rest by another small pendulum (brake system).

A pendulum extension was attached to the pendulum and the ATD head. The pendulum extension was free to oscillate, and a chain connected the pendulum center to the end of the

pendulum extension. The purpose of the chain was to maintain the head and pendulum in a straight line and prevented the extension from hitting the bulkhead. Tests with the pendulum rig could be conducted in two different configurations. In the first configuration, the ATD head was loosely attached to the pendulum. The pendulum was raised to the desired height and released to strike the test target at the desired velocity. In the other configuration, a panel with padding material was fixed loosely to the pendulum, raised to the desired height, and released to strike the seated dummy. Suitably adjusting the inclination of the pendulum and allowing it to fall freely under gravity could achieve any desired impact velocity. The pendulum had the advantages of being simple and flexible in operation. With a pendulum test setup, both the padding material and the individual body components could be evaluated. This may be used for simulating the impact of an occupant onto the interior structure or the impact on a pedestrian. The effect of padding material stiffness on the HIC value may be analyzed; and a model of head impact, using nonlinear stiffness and damping properties, can be developed. This helps in the selection of an optimum material for reducing severe head injuries. The HIC values obtained for heavier masses did not correlate with the sled test results.

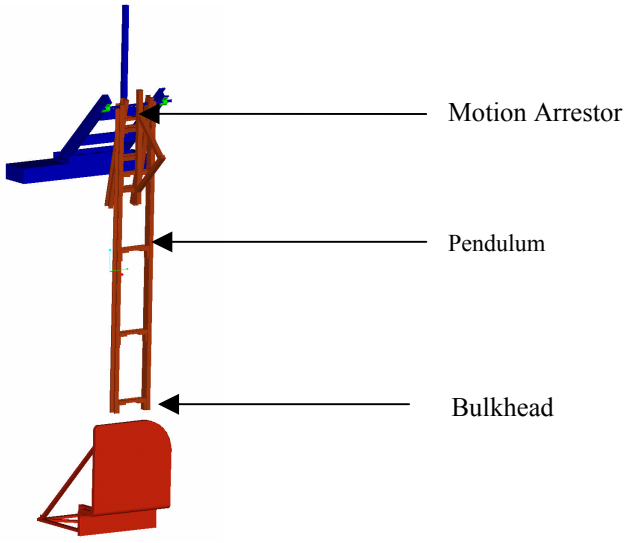

FIGURE A-4. PENDULUM RIG TESTER

A.5 REFERENCES.

A-1. Van Gowdy, "Evaluation of the Instrumented Ball Impact Procedure to Assess Head Impact Protection in Airplanes," SAE Technical Paper 951166.

A-2. Saul A. Roger, Farson Max, and Guenther A. Dennis, "Development of a Component Level Head Impact Test Device," SAE Paper No. 861889, October 1986.

A-3. Lankarani, H.M, Hooper, S.J, and Mirza, M.C, "An Evaluation of a Component HIC Apparatus," National Institute for Aviation Research, Wichita State University, August 1998.

APPENDIX B—DATA SHEETS FOR SLED TESTS

Summary sheets showing the velocity and acceleration plots along with results are tabulated for each full-scale sled test. Data sheets for the sled tests follow.

DATA SHEET FOR SLED TEST 97191-02

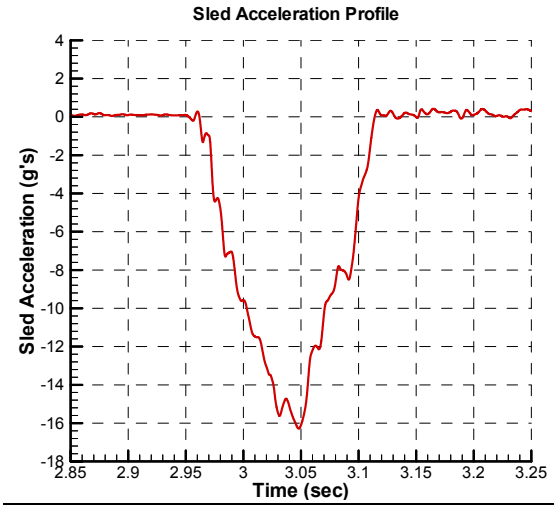

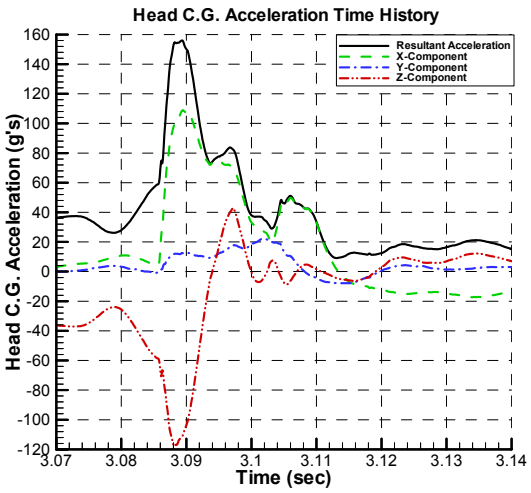

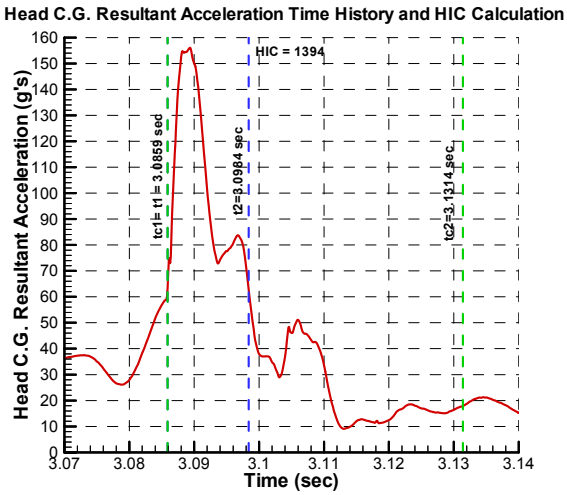

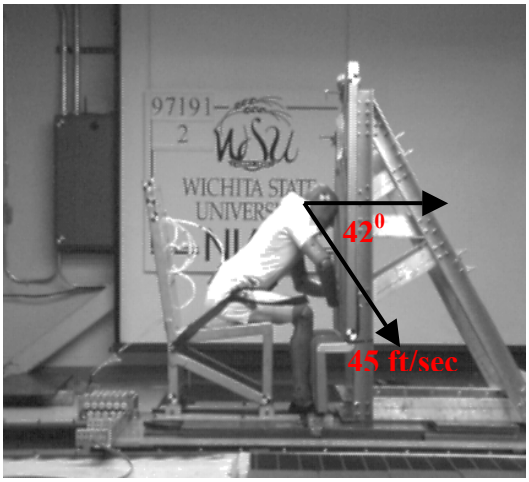

Results of Sled Test 97191–02

Bulkhead	-	Simulated bulkhead (cabin class divider)
Seat Set back distance (in.)	-	35
Peak Sled Deceleration (g's)	-	16.3
Frame Zero (sec)	-	3.0619
Head Impact Velocity (ft/sec)	-	45
Head Impact Angle (deg.)	-	42
Head c.g. peak resultant accel. (g's)	-	156
Head c.g. average resultant accel. (g's)	-	104.1
HIC	-	1394
$\Delta t = t_2 - t_1$ (ms)	-	12.5 (t_1 = 3.0859 sec, t_2 = 3.0984 sec)
Contact Start Time, tc_1 (sec)	-	3.0859
Contact End Time, tc_2 (sec)	-	3.1314

DATA SHEET FOR SLED TEST 99109-02

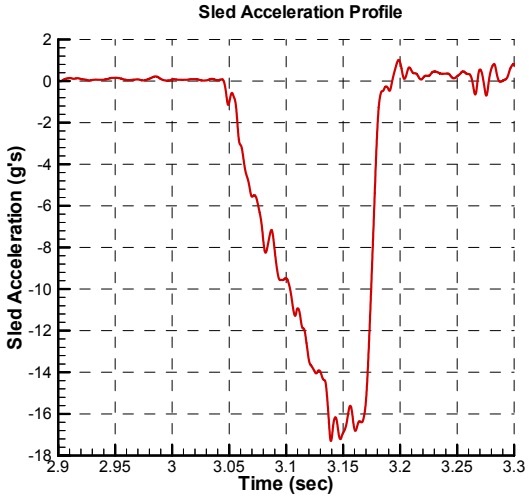

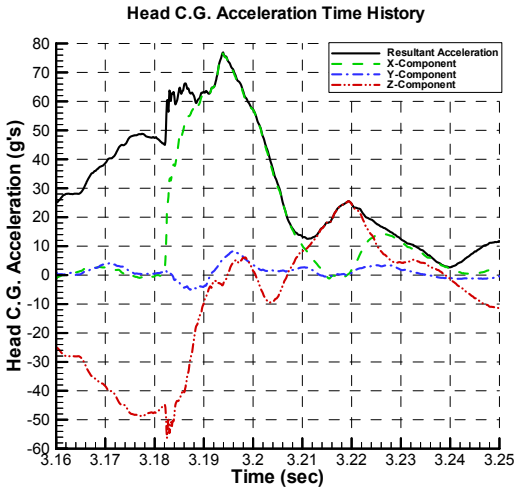

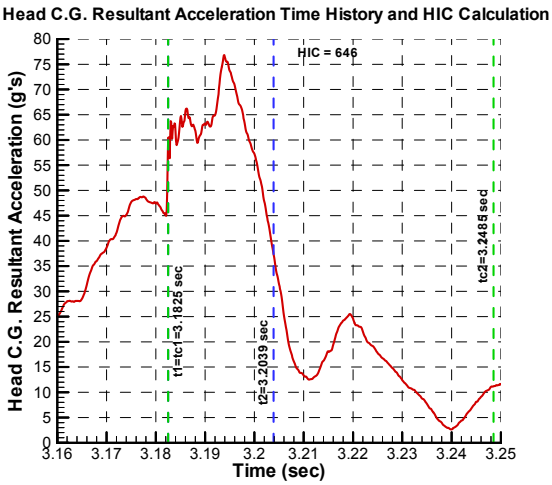

Results of Sled Test 99109–02

Bulkhead	-	Simulated bulkhead (slitted cabin class divider)
Seat Set back distance (in.)	-	35
Peak Sled Deceleration (g's)	-	17.3
Frame Zero (sec)	-	3.1025
Head Impact Velocity (ft/sec)	-	46
Head Impact Angle (deg.)	-	39
Head c.g. peak resultant accel. (g's)	-	77
Head c.g. average resultant accel. (g's)	-	61.8
HIC	-	646
$\Delta t = t_2 - t_1$ (ms)	-	21.4 (t_1 = 3.1825 sec, t_2 = 3.2039 sec)
Contact Start Time, tc_1 (sec)	-	3.1825
Contact End Time, tc_2 (sec)	-	3.2485

DATA SHEET FOR SLED TEST 99137-02

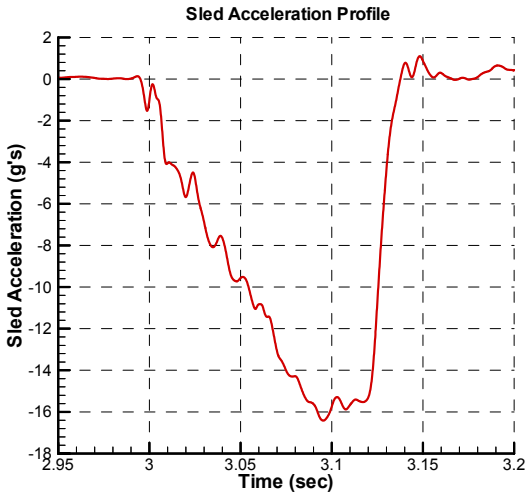

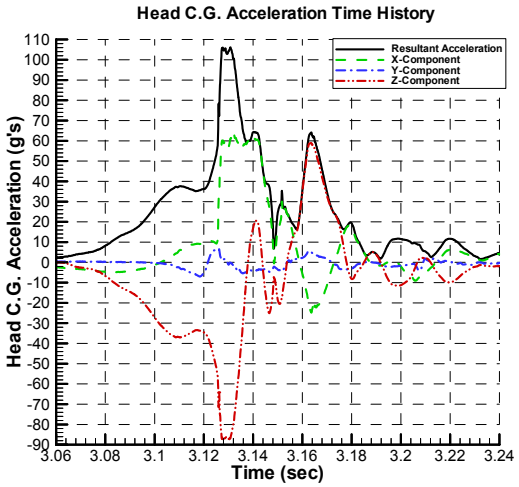

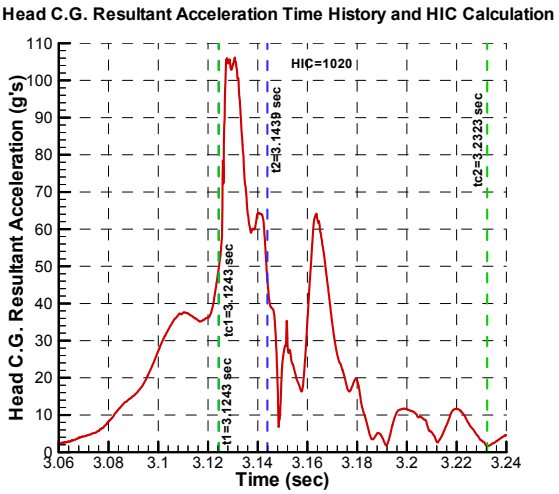

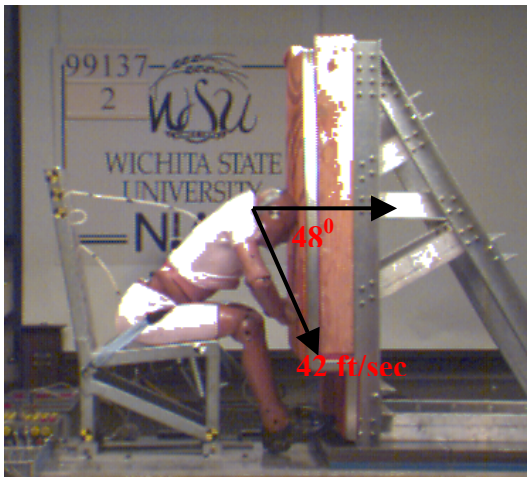

Results of Sled Test 99137–02

Bulkhead	-	Simulated bulkhead (slitted cabin class divider)
Seat Set back distance (in.)	-	35
Peak Sled Deceleration (g's)	-	16.4
Frame Zero (sec)	-	3.1243
Head Impact Velocity (ft/sec)	-	42
Head Impact Angle (deg.)	-	48
Head c.g. peak resultant accel. (g's)	-	106
Head c.g. average resultant accel. (g's)	-	77
HIC	-	1020
$\Delta t = t_2 - t_1$ (ms)	-	19.6 (t_1 = 3.1243 sec, t_2 = 3.1439 sec)
Contact Start Time, tc_1 (sec)	-	3.1243
Contact End Time, tc_2 (sec)	-	3.2323

DATA SHEET FOR SLED TEST 96288-004

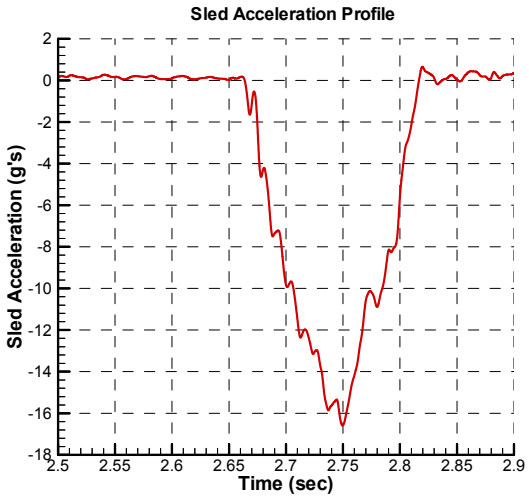

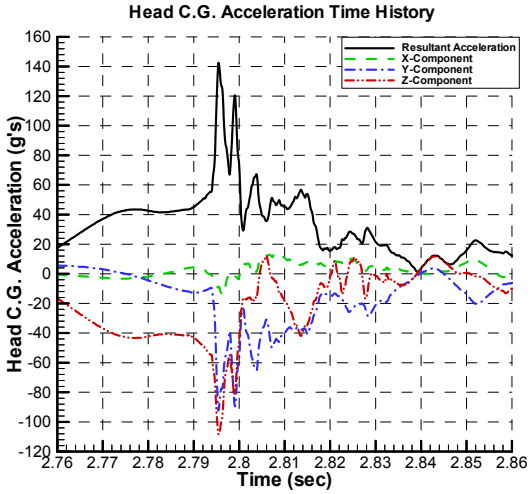

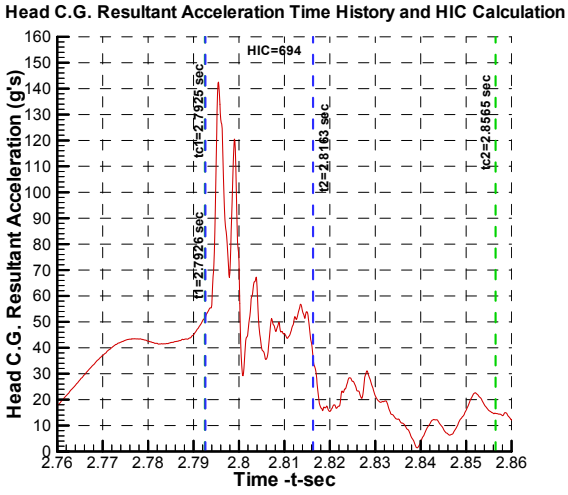

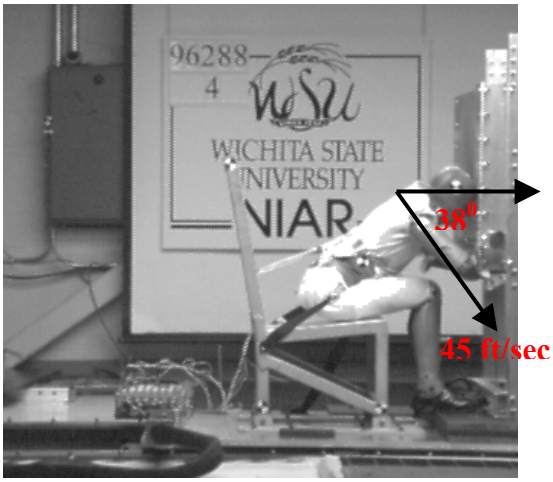

Results of Sled Test 96288-004

Bulkhead	-	0.063-in.-thick Al 2024 T3, 28.5 x 31 in.
Seat Set back distance (in.)	-	35
Peak Sled Deceleration (g's)	-	16.6
Frame Zero (sec)	-	2.6745
Head Impact Velocity (ft/sec)	-	45
Head Impact Angle (deg.)	-	38
Head c.g. peak resultant accel. (g's)	-	142.5
Head c.g. average resultant accel. (g's)	-	61
HIC	-	694
$\Delta t = t_2 - t_1$ (ms)	-	23.7 (t_1 = 2.7926 sec, t_2 = 2.8163 sec)
Contact Start Time, tc_1 (sec)	-	2.7925
Contact End Time, tc_2 (sec)	-	2.8565

DATA SHEET FOR SLED TEST 01008-8

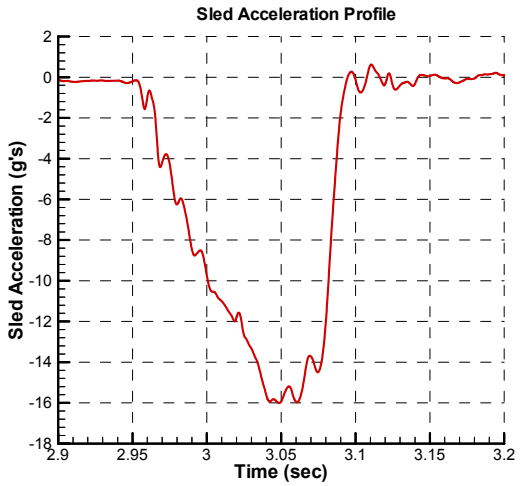

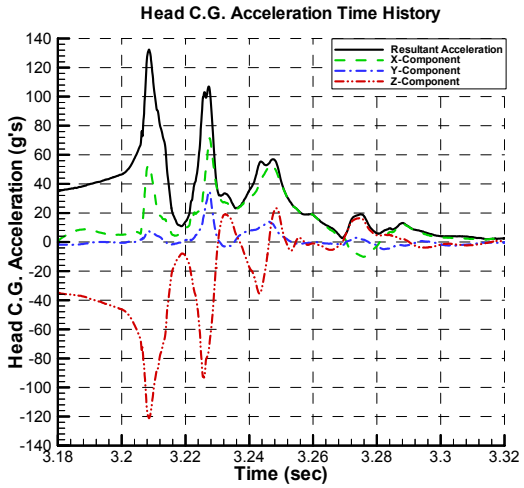

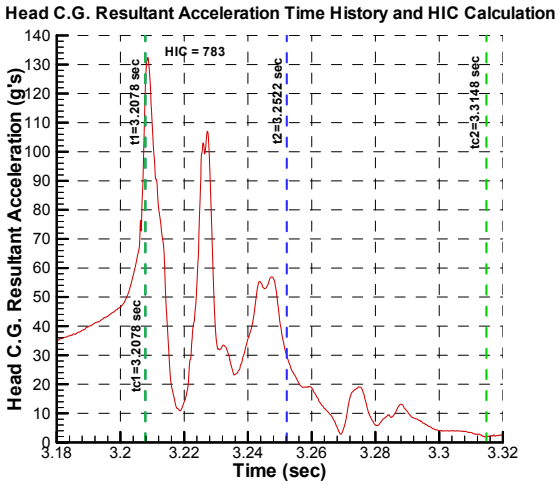

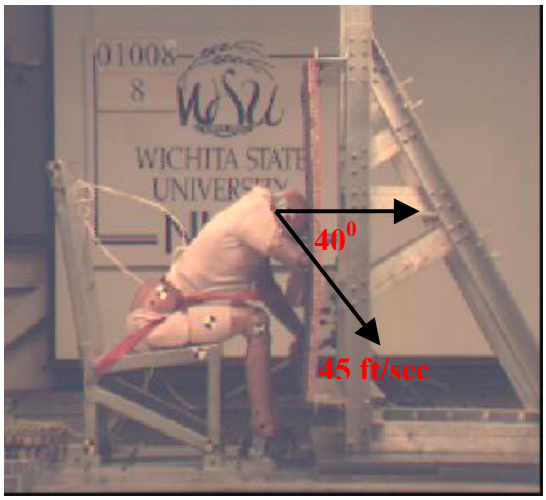

Results of Sled Test 01008-8

Bulkhead	-	Nomex honeycomb panel, 1inch thick with fiberglass sheets and carpet
Seat Set back distance (in.)	-	35
Peak Sled Deceleration (g's)	-	16
Frame Zero (sec)	-	3.1648
Head Impact Velocity (ft/sec)	-	45
Head Impact Angle (deg.)	-	40
Head c.g. peak resultant accel. (g's)	-	132.4
Head c.g. average resultant accel. (g's)	-	50
HIC	-	783
$\Delta t = t_2 - t_1$ (ms)	-	44.4 (t_1 = 3.2078 sec, t_2 = 3.2522 sec)
Contact Start Time, tc_1 (sec)	-	3.2078
Contact End Time, tc_2 (sec)	-	3.3148

APPENDIX C—ENGINEERING DRAWINGS OF HCT

The following engineering drawings were made using Pro-Engineer 2000i^2:

ASSEMBLY OF COMPONENT HIC TESTER (MODE I)

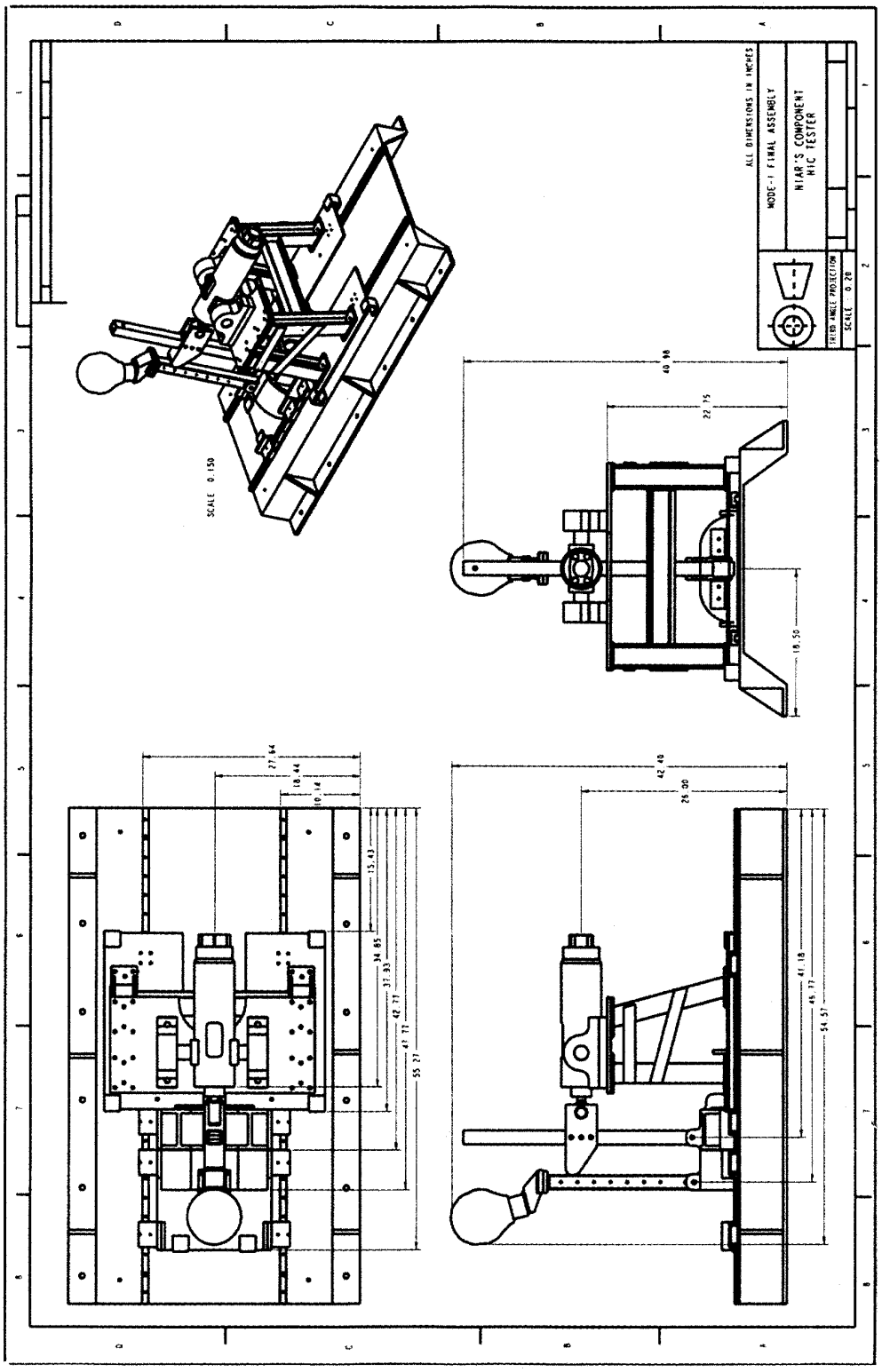

ASSEMBLY OF COMPONENT HIC TESTER (MODE II)

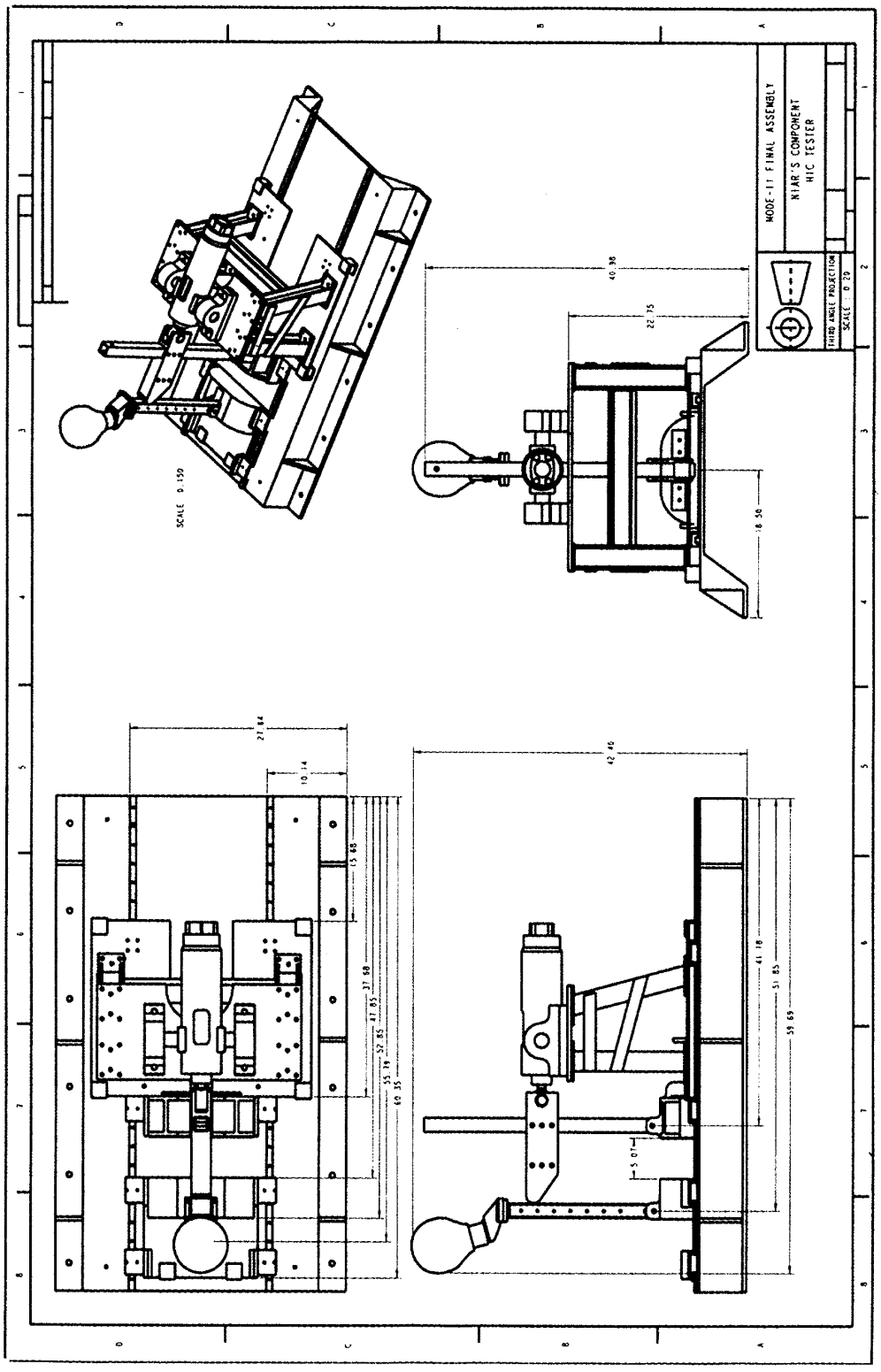

BASE PLATE

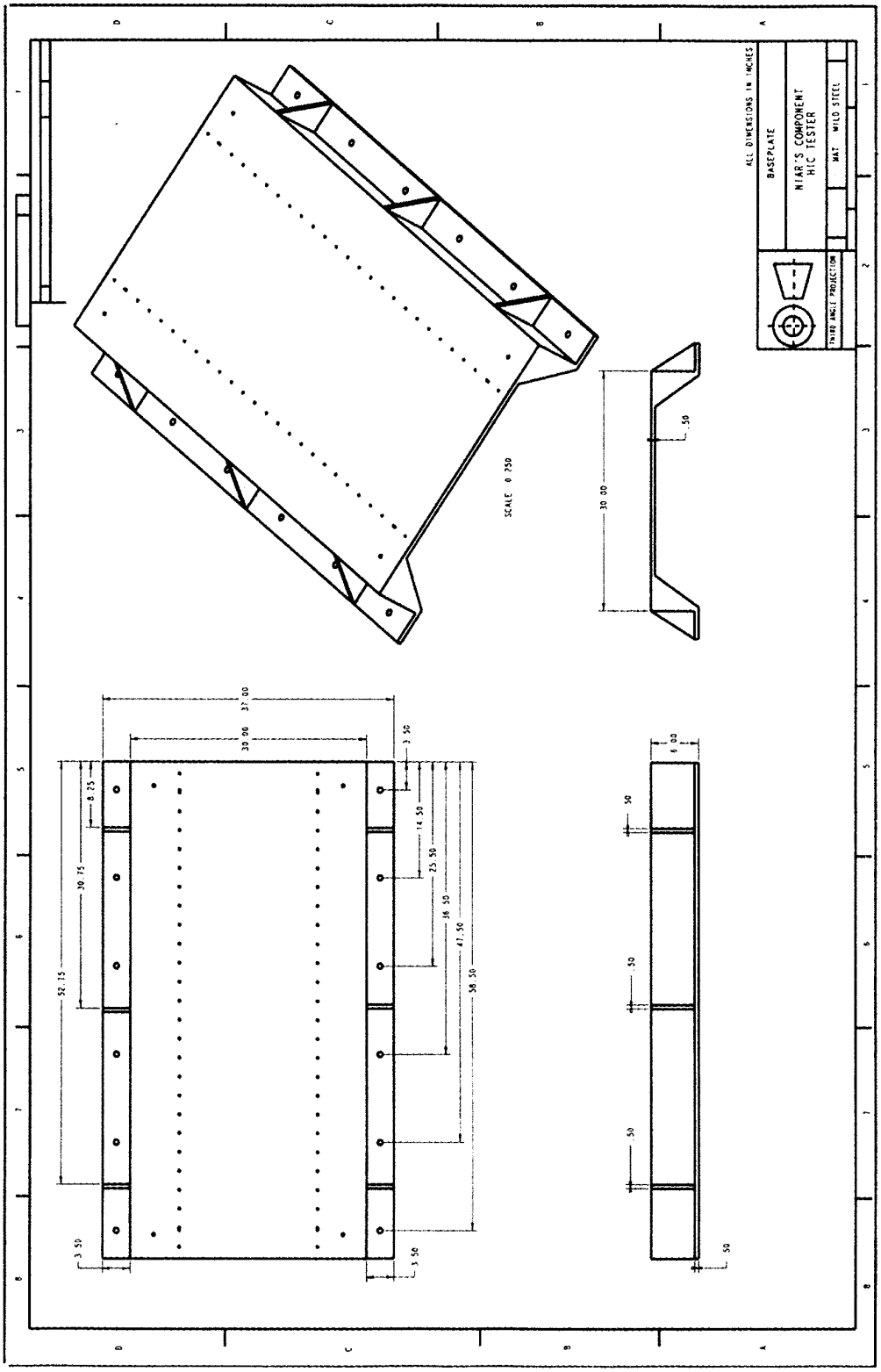
ALL DIMENSIONS IN INCHES
BASEPLATE
NHAR'S COMPONENT
HIC TESTER
MAT MILD STEEL
THIRD ANGLE PROJECTION
SCALE 0.250
30.00
.50
32.00
30.00
3.50
8.75
30.75
52.75
14.50
25.50
36.50
47.50
58.50
3.50
3.50
6.00
.50
.50
.50
.50

ACTUATOR PLATE

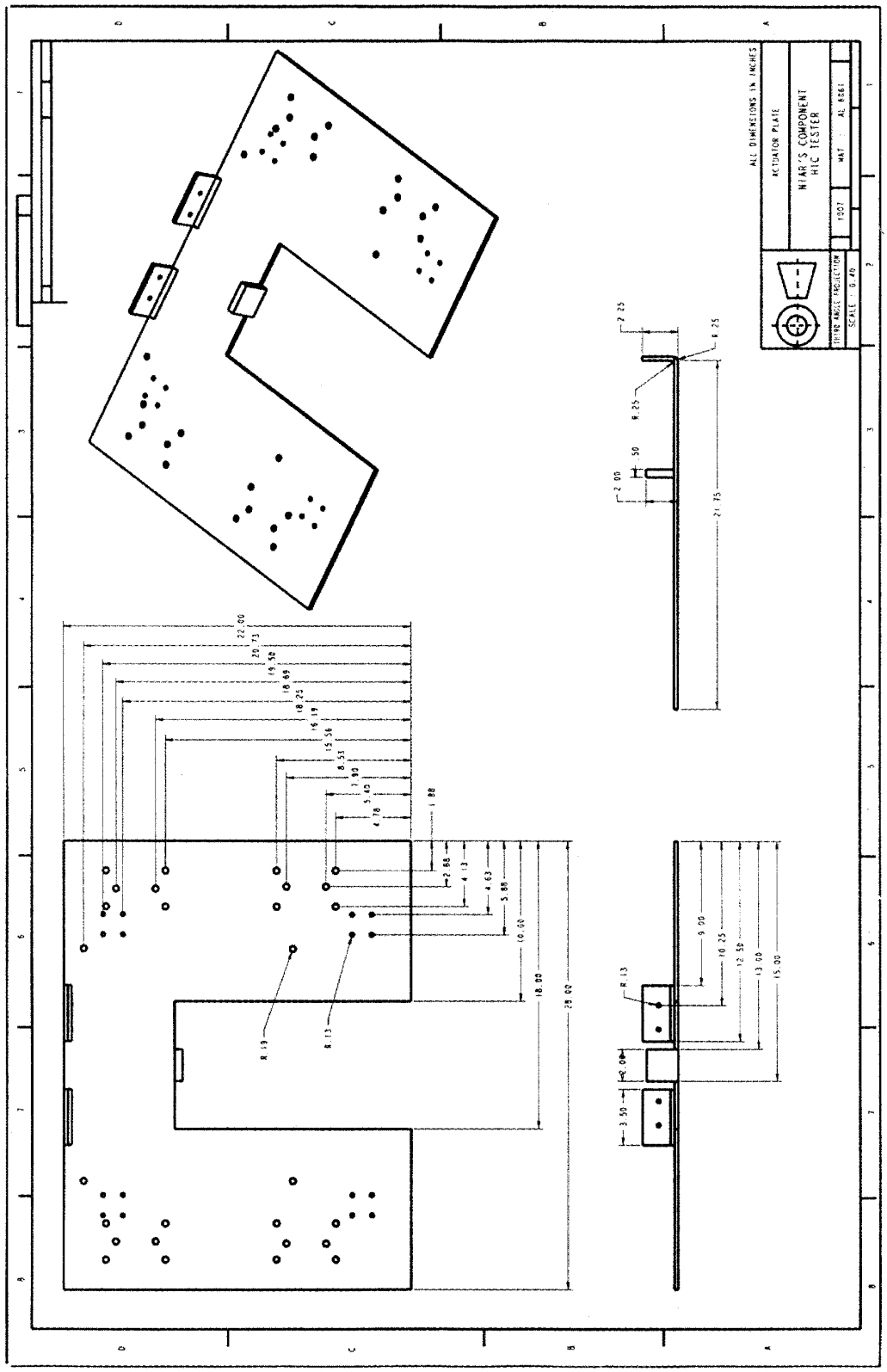

STAND ASSEMBLY

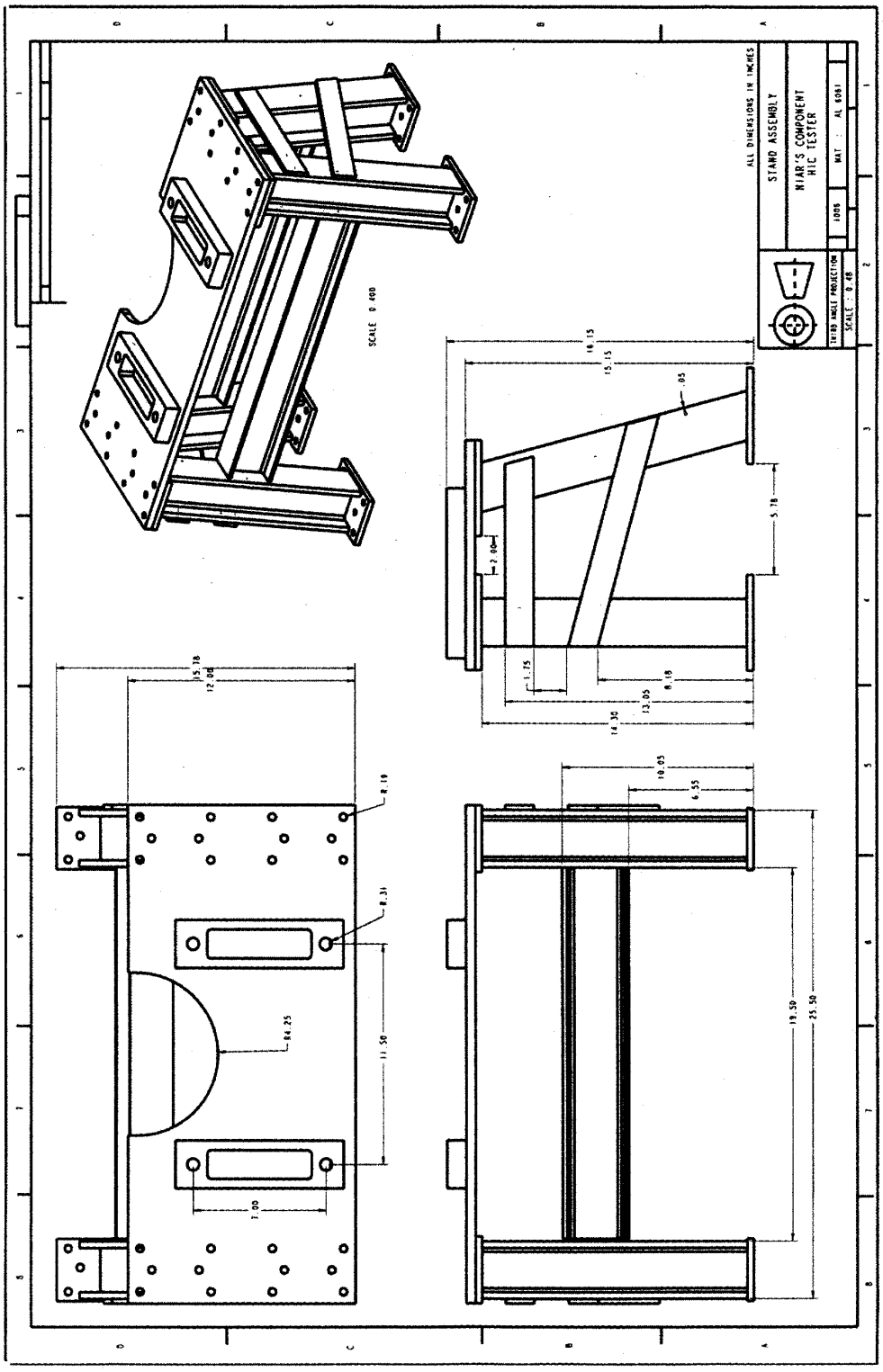

LOWER TORSO

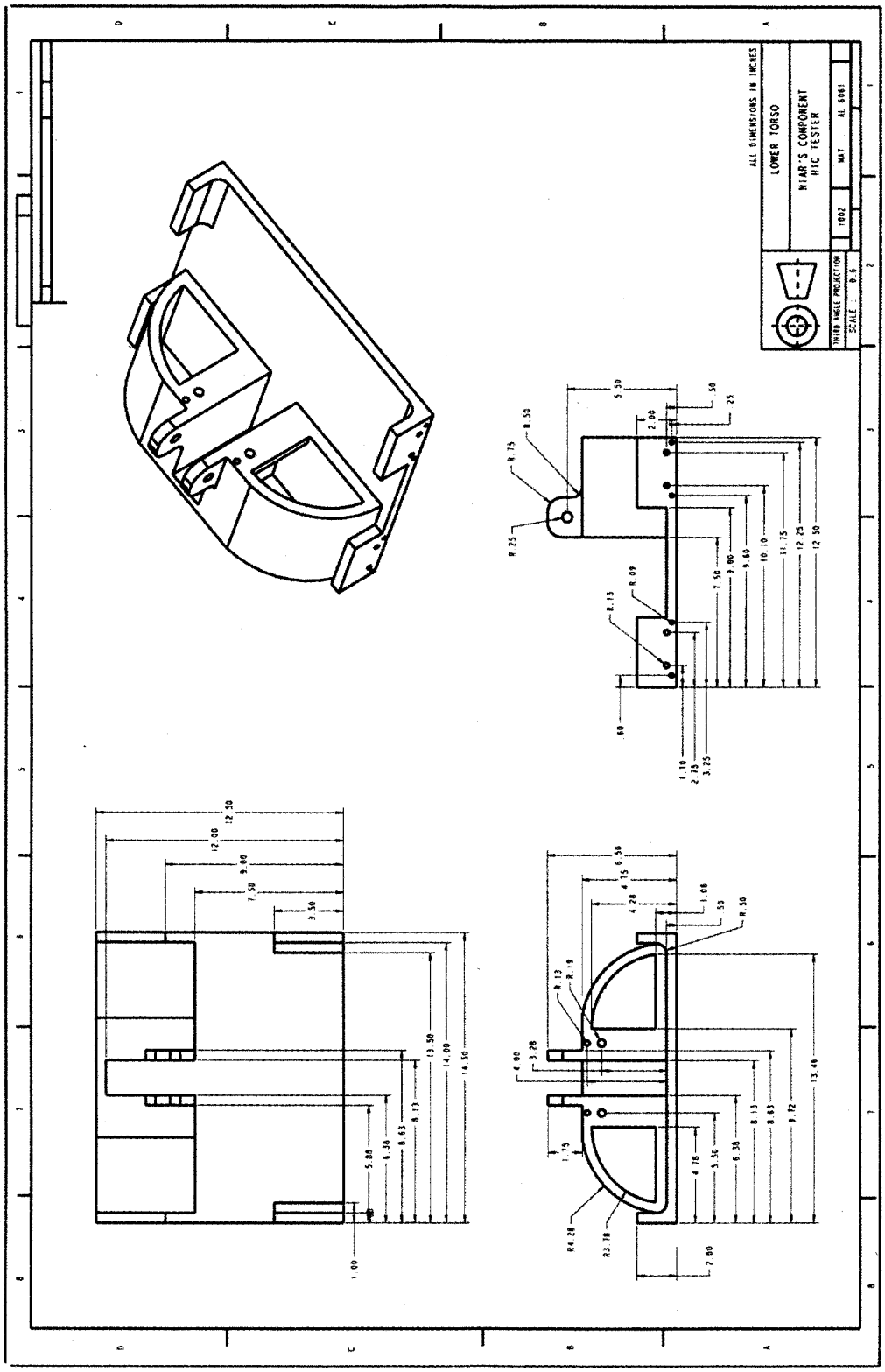
ALL DIMENSIONS IN INCHES
LOWER TORSO
NHTSA'S COMPONENT
HIC TESTER
1002
MAT
AL 6061
THIRD ANGLE PROJECTION
SCALE
D.S

PENDULUM ARM

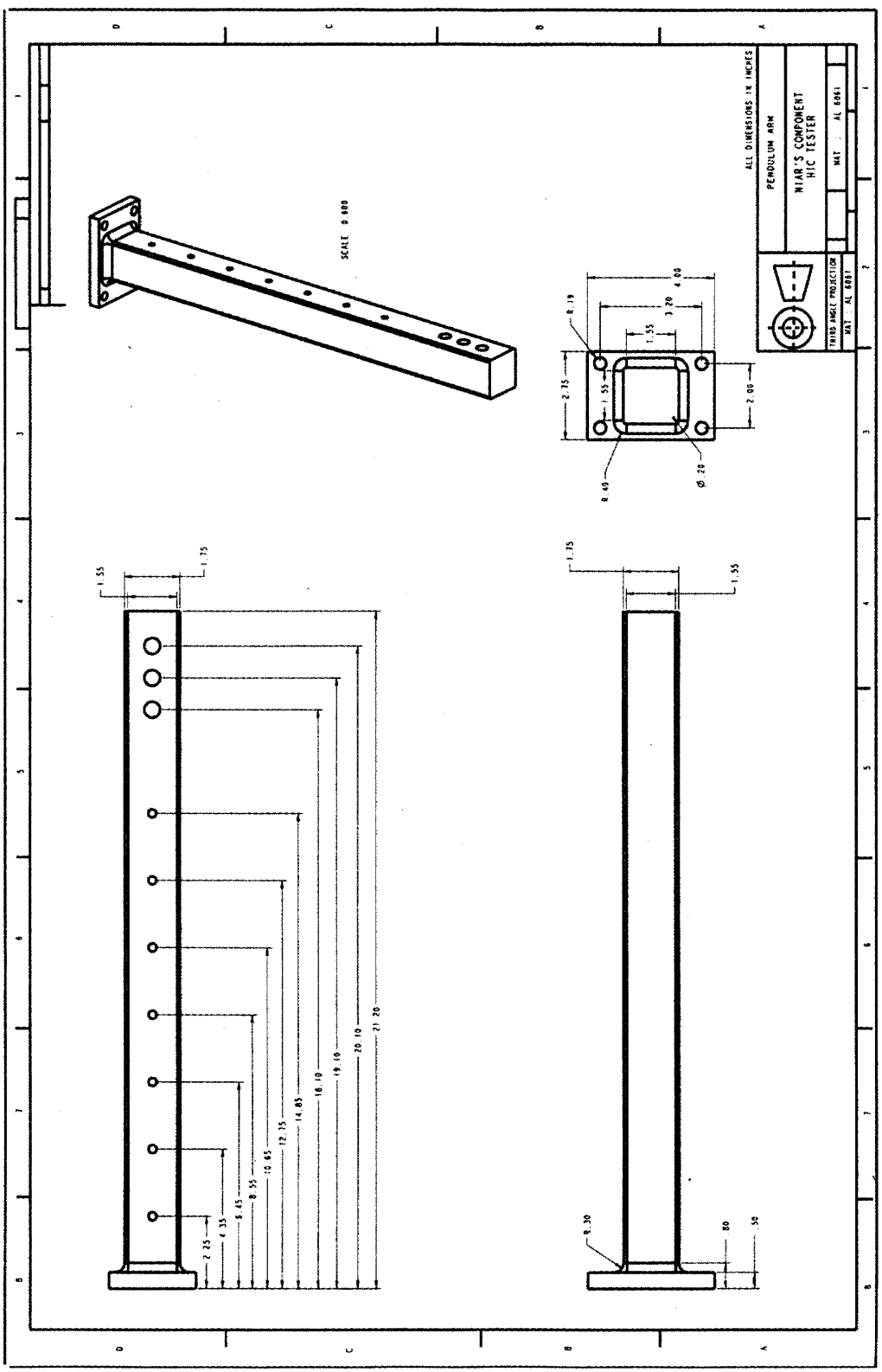

NECK BRACKET

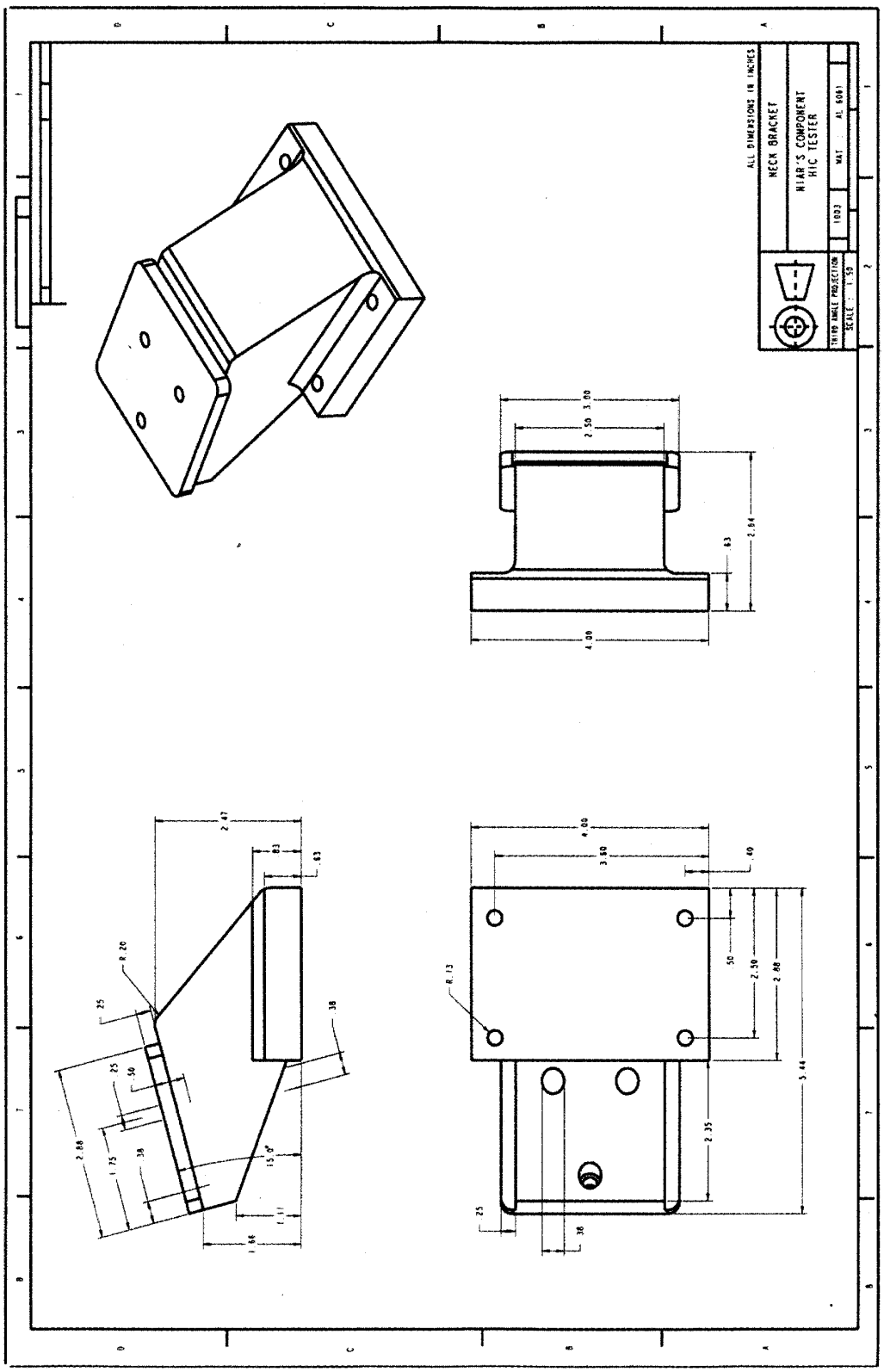

SUPPORT ARM PIVOT BASE

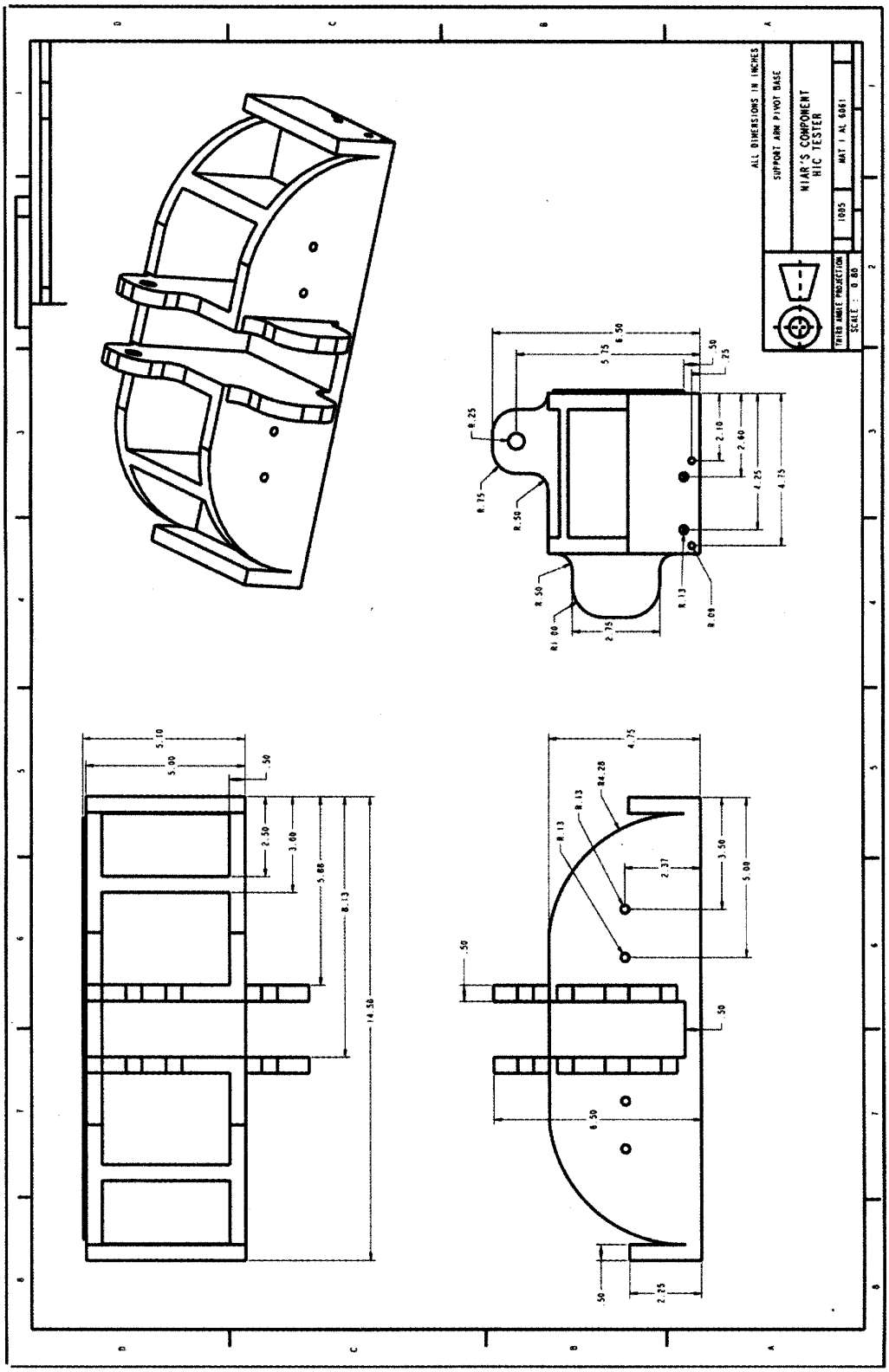

SUPPORT ARM

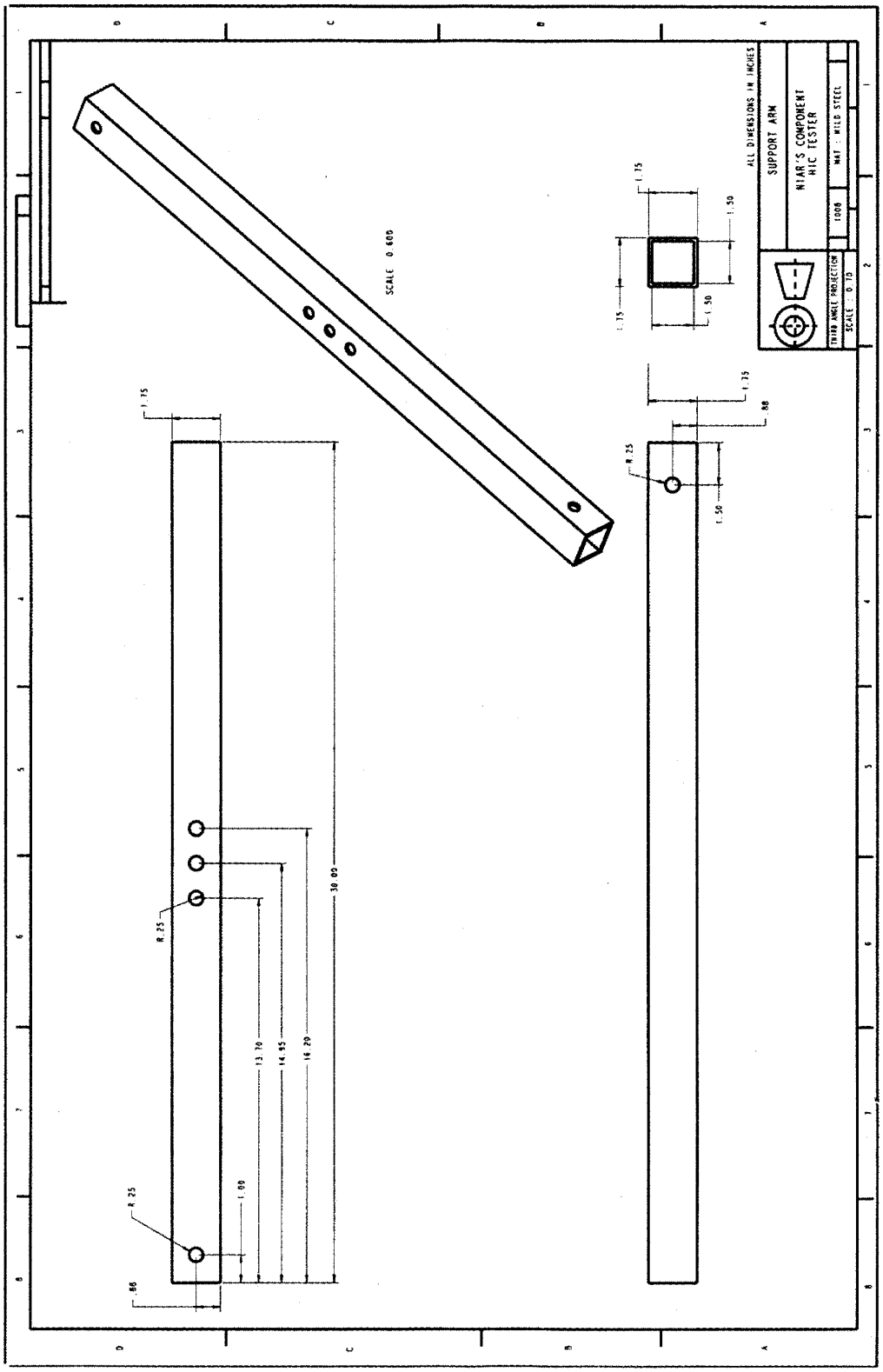
ALL DIMENSIONS IN INCHES
SUPPORT ARM
NIAR'S COMPONENT
HIC TESTER
1000
MAT : MILD STEEL
THIRD ANGLE PROJECTION
SCALE : 0.10
SCALE 0.600
1.75
1.50
1.75
1.50
1.75
.88
R.25
1.50
1.75
R.25
30.00
13.70
14.45
16.20
R.25
1.00
.86

SUPPORT ARM EXTENSION (MODE I)

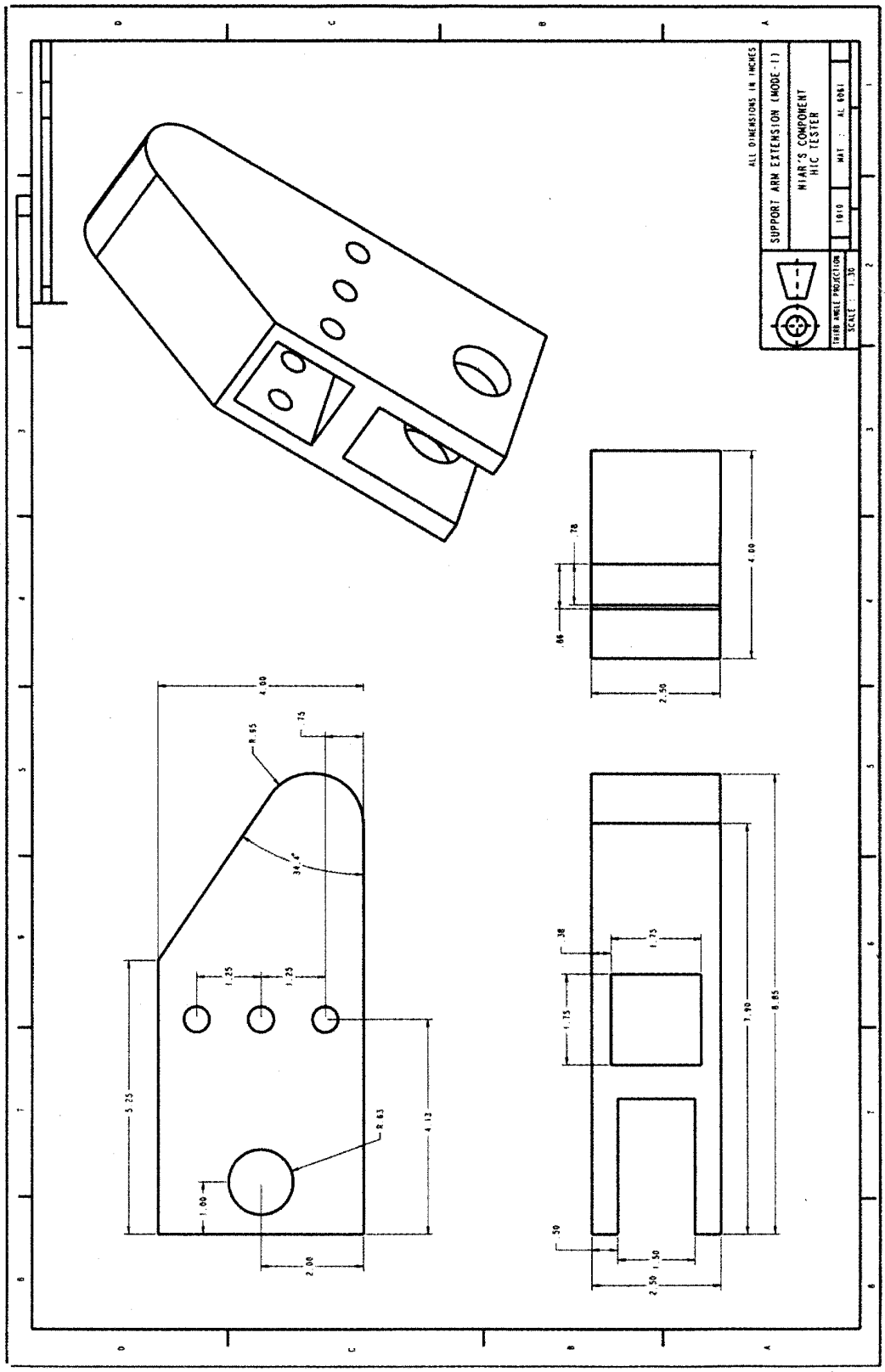

SUPPORT ARM EXTENSION (MODE II)

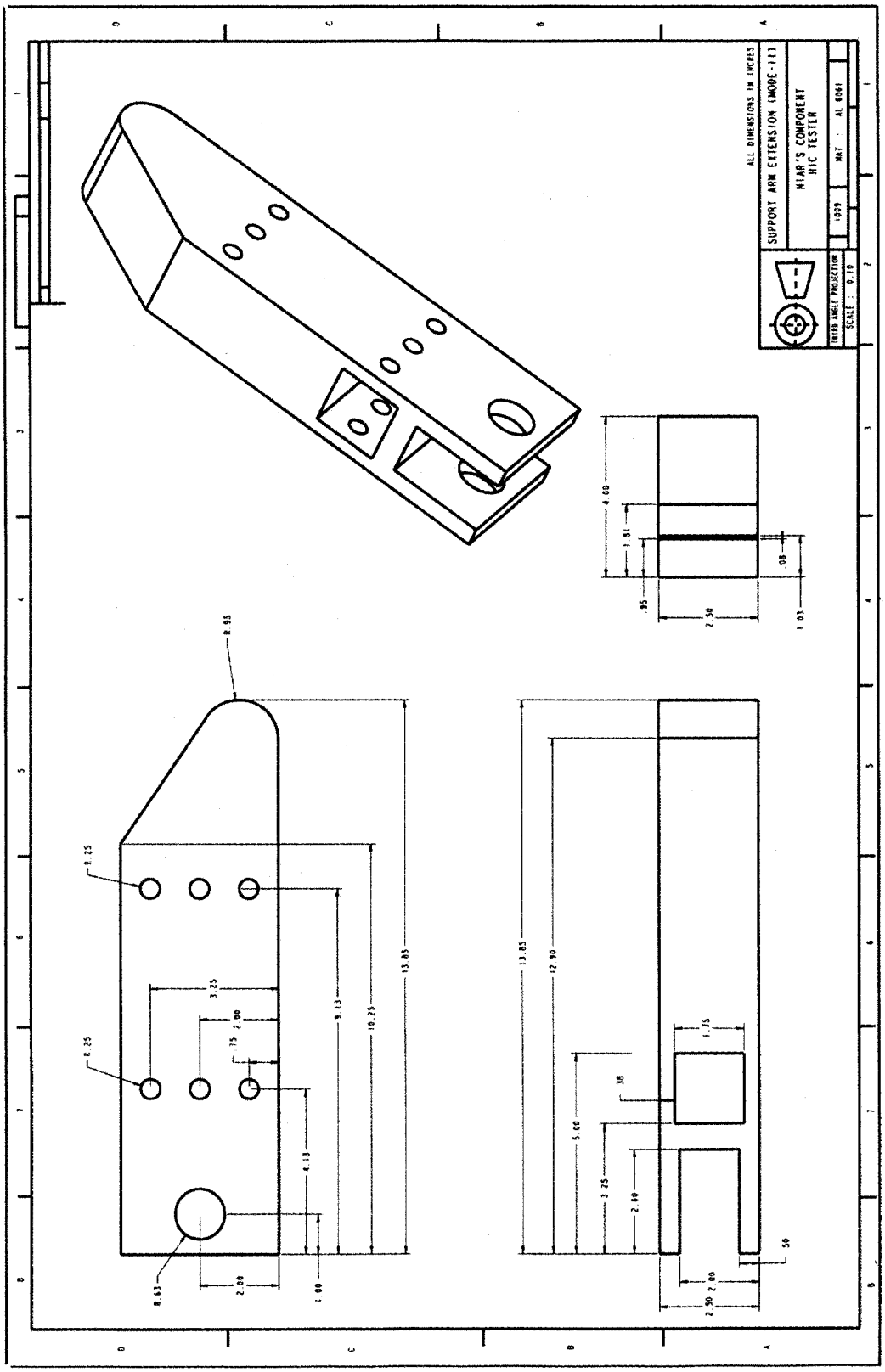

APPENDIX D—PROPULSION SYSTEM

Figure D-1 shows the schematic representation of the propulsion system. The propulsion system allows high-pressure nitrogen gas stored in the accumulator to be discharged instantaneously through an actuator, providing angular velocity to the pendulum arm.

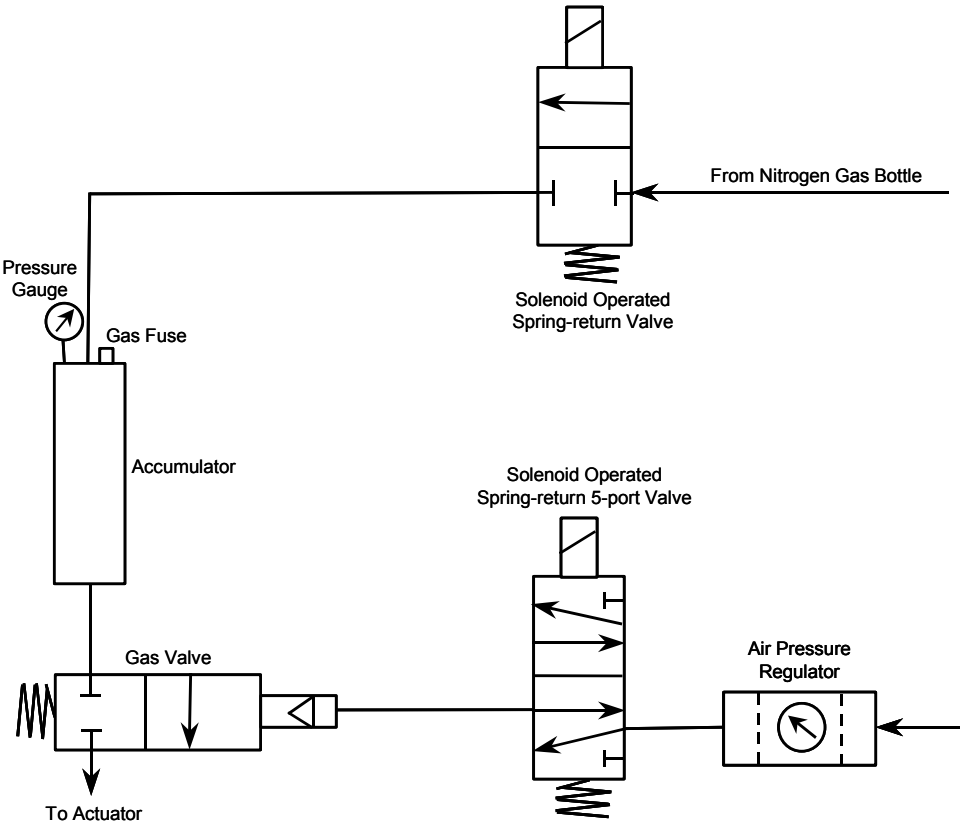

FIGURE D-1. SCHEMATIC REPRESENTATION OF PROPULSION SYSTEM

The nitrogen gas bottle is plumbed to a solenoid shutoff valve and then to the accumulator. The accumulator is charged to the desired operating pressure by opening the solenoid shutoff valve and the pressure regulator mounted on the nitrogen bottle, after which both are closed. The accumulator pressure controls the output force of the actuator and, therefore, the velocity of the pendulum arm. Triggering the solenoid-operated, 5-port valve causes compressed air, set at 60 psi, to open the gas valve allowing the accumulator to discharge through the actuator. The actuator piston travels down the actuator cylinder and provides angular velocity to the pendulum arm via the support arm assembly. The compressed nitrogen gas in the actuator cylinder is vented into the atmosphere through the longitudinal slot provided at the end of the cylinder. Figure D-2 shows the components of the propulsion system.

The maximum pressure that can be maintained in the accumulator is 600 psi. The accumulator is provided with a gas fuse to vent out excess pressure. The accumulator and the gas valve are fixed rigidly to withstand the high forces generated during the system operation. Figure D-3 shows the actuator assembly.

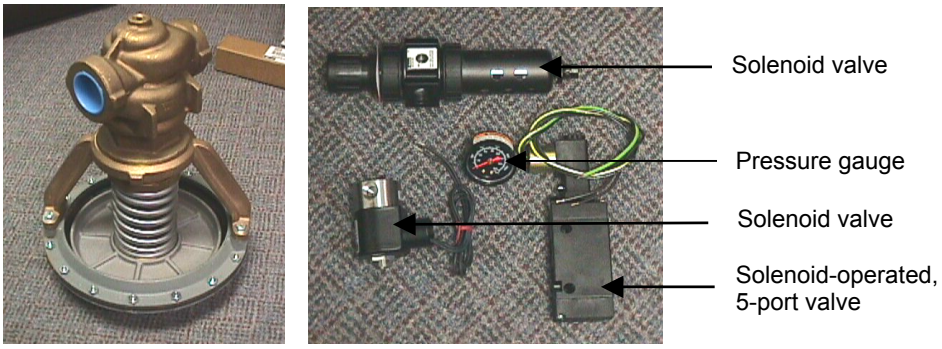

(a) Gas Valve (b) Control Accessories

(c) Accumulator

FIGURE D-2. PROPULSION SYSTEM COMPONENTS

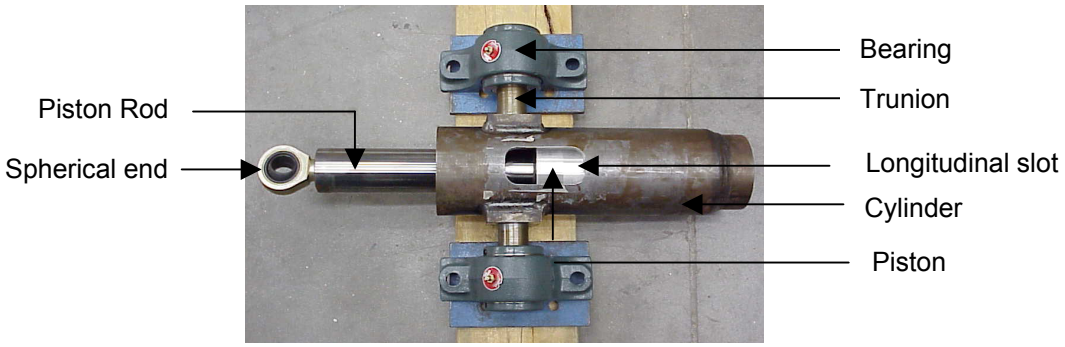

FIGURE D-3. ACTUATOR ASSEMBLY

The cylinder length is 20 inches with a 4-inch bore, an 8-inch active stroke, and a 2-inch-diameter piston. The cylinder bore and the piston outer surface are machined to high tolerences and low friction seals are used at the ends of the cylinder to increase efficiency. The piston is designed to withstand high pressure, speed, and temperature and is made of Aluminum-6065. One end of the piston rod is connected to the piston and the other end to a threaded spherical end. The spherical end is connected to the support arm assembly and transfers the force from the actuator to the pendulum arm. The cylinder has a longitudinal slot, 1 1/2 inches wide and 4 inches long to vent the gas. The edges of the slot are rounded to reduce the stress concentration. The actuator trunion point is mounted on the stand with a set of 75-mm bore type-e bearings. The bearings are capable of withstanding high loads and are mounted on the stand with 3/4-inch-diameter bolts.

APPENDIX E—PRESSURE-VELOCITY CALIBRATION TESTS

The component head injury criteria (HIC) tester was calibrated for a given head impact velocity by setting the actuator pressure at a predetermined value to achieve the desired head impact velocity. A series of tests were conducted with varying actuator pressure and fixed head impact angle. A generalized relationship between actuator pressure and head impact velocity was obtained. The procedure was as follows.

E.1 TEST METHODOLOGY.

The bulkhead material used for the entire test series was an aluminum sheet (2024-T3, 0.063 in. thick). Figure E-1 shows the dimensions of the aluminum bulkhead and fixture details.

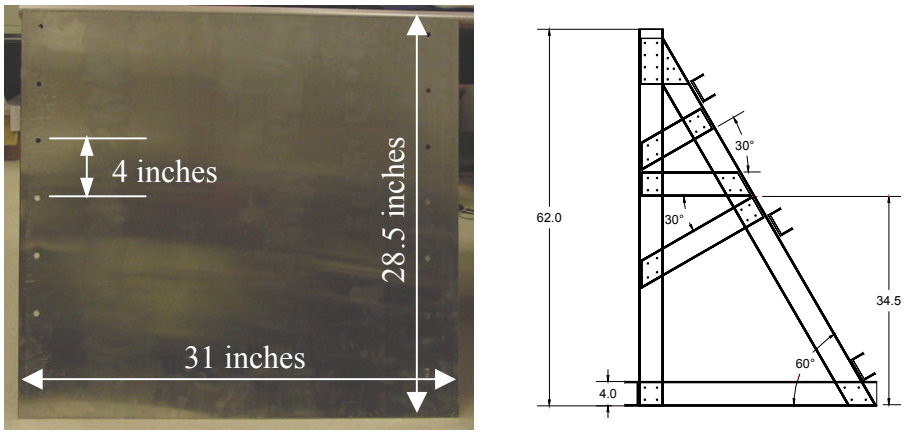

FIGURE E-1. ALUMINUM BULKHEAD AND FIXTURE DETAILS

Tests were conducted with head impact angles in the range of 35-60 degrees in increments of 5 degrees. For each head impact angle, the actuator pressure was varied and head impact velocity obtained from video data. The head impact angle, actuator pressure, and pivot-point distance from the bulkhead were measured and recorded. The bulkhead was positioned such that the head impacted at the bulkhead center.

Figure E-2 shows the operating methodology of the component HIC tester. The head impact angle and the impact location on the bulkhead were set prior to each test by positioning the bulkhead. The actuator pressure for each head impact angle was selected in the range of 70-150 psi. The data acquisition system and the high-speed video capturing devices were set to record head acceleration data and the video. The accumulator discharges and actuates the cylinder piston. Raw data obtained from the data acquisition system was analyzed for each test and head impact velocity calculated. The data obtained from each test for a given head impact angle is plotted and a linear expression for actuator pressure versus head impact velocity was obtained.

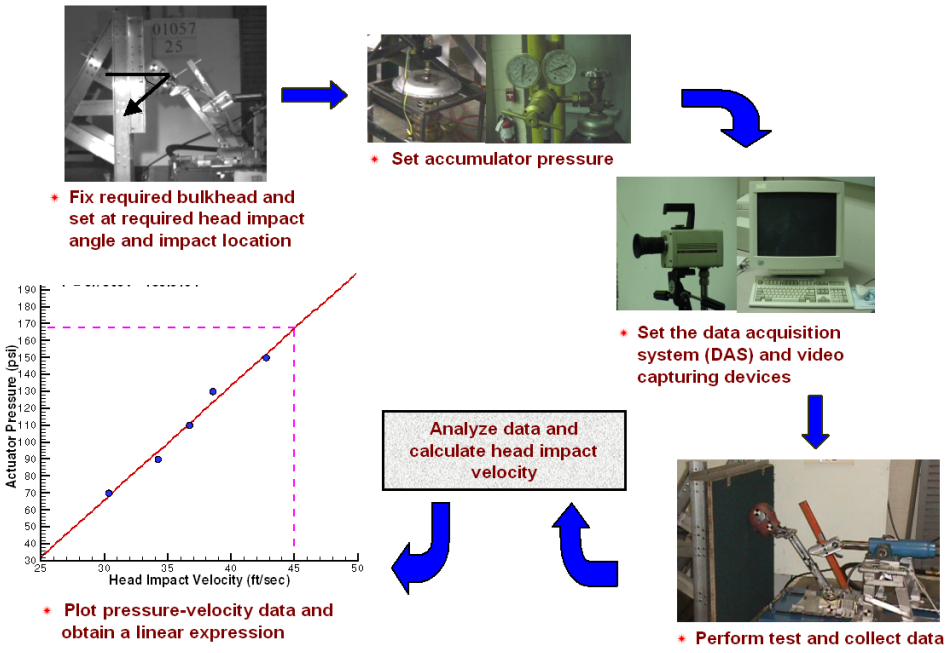

FIGURE E-2. PRESSURE VS VELOCITY CALIBRATION

The results obtained from each calibration test are tabulated in table E-1. Figure E-3 shows the pressure-velocity plot from data analysis.

TABLE E-1. PRESSURE VS VELOCITY CALIBRATION DATA

Test 01204 -	Head Impact Angle (deg.)	Actuator Pressure (psi)	Head Impact Velocity (ft/sec)
04	35	110	34.7
05	35	130	38.6
26*	35	150	39.3
08	40	70	30.9
09	40	90	32.5
10	40	120	39.5
11	40	130	40.5
12	40	150	41.3
13	45	70	30.3
14	45	90	34.2
15	45	110	36.7
16	45	130	38.6
17	45	150	42.7
18	50	70	30.9
19	50	90	33.8
20	50	110	37.8

TABLE E-1. PRESSURE VS VELOCITY CALIBRATION DATA (Continued)

Test 01204 -	Head Impact Angle (deg.)	Actuator Pressure (psi)	Head Impact Velocity (ft/sec)
21	50	130	38.3
22	50	150	41.2
28	55	80	31.0
29	55	90	32.8
30	55	110	35.8
31	55	130	38.7
32	55	150	41.8
23	60	70	29.8
24	60	90	34.1
25	60	110	35.4
26	60	130	36.9
27	60	150	40.6

* Test 01057-26

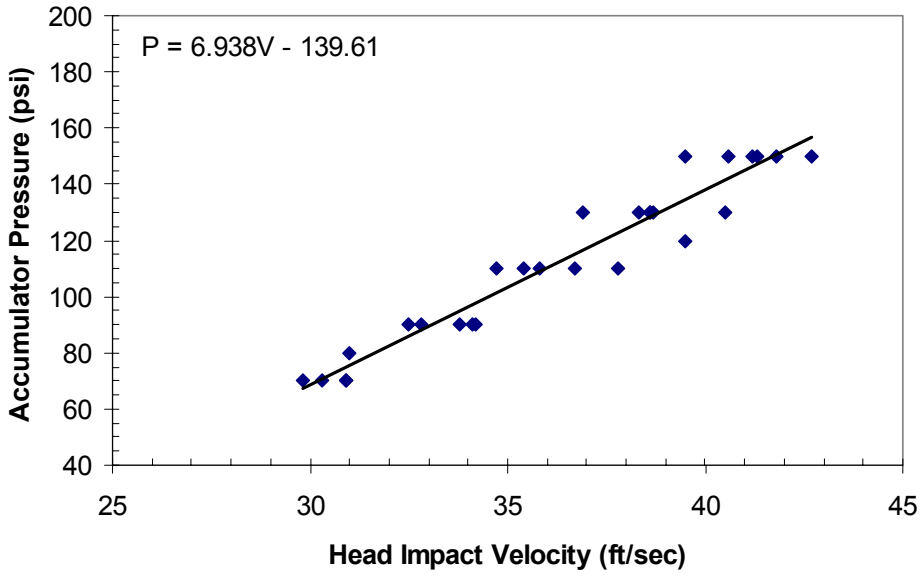

FIGURE E-3. PRESSURE VS VELOCITY PLOTS

APPENDIX F—DATA SHEETS FOR HCT TESTS

Data sheets for the HCT tests follow.

DATA SHEET FOR HCT TEST 01057-24

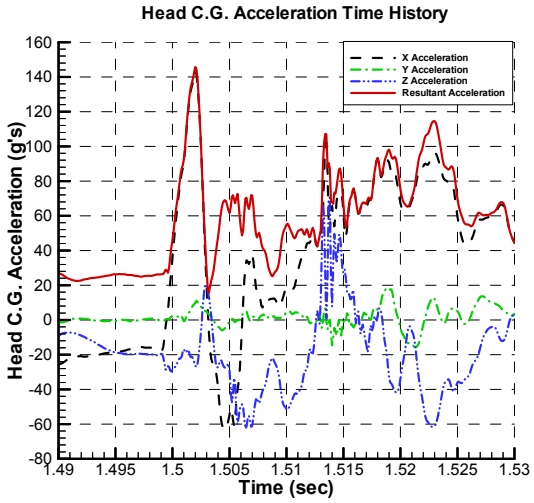

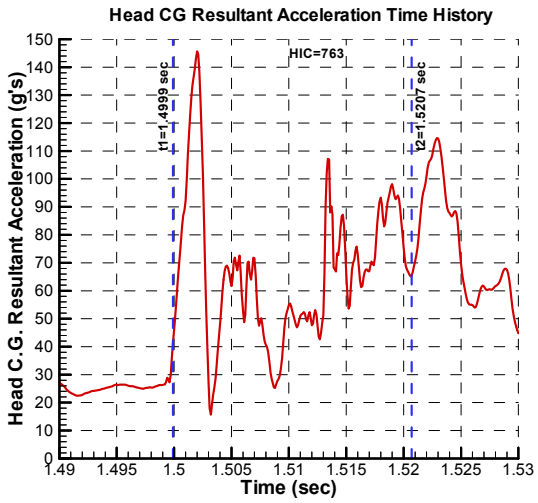

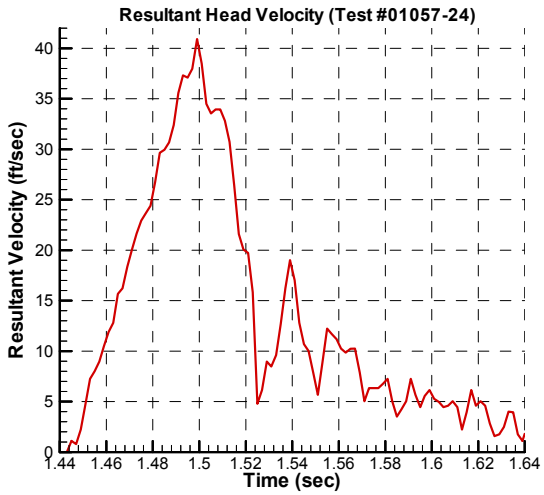

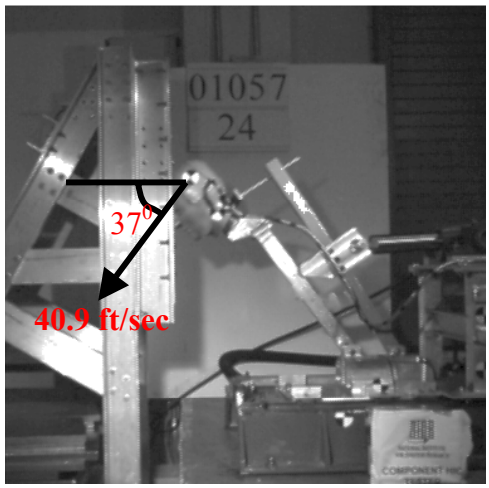

Results of Component HIC Test 01057-24

Bulkhead type	-	0.063-in.-thick Al 2024-T3, 28.5 x 31 in.
Pivot Point setback distance (in.)	-	22.5
Operating Pressure (psi)	-	150
Pendulum Type	-	Al 6061-T6, 7 lbs
Frame Zero (sec)	-	1.6429
Head Impact Velocity (ft/sec)	-	40.9
Head Impact Angle (deg.)	-	37
Head c.g. peak resultant accel. (g's)	-	145.6
Head c.g. average resultant accel. (g's)	-	67
HIC	-	763
$\Delta t = t_2 - t_1$ (ms)	-	20.8 (t_1 = 1.4999 sec, t_2 = 1.5207 sec)
Contact Start Time, tc_1 (sec)	-	1.4989
Contact End Time, tc_2 (sec)	-	1.5209

DATA SHEET FOR HCT TEST 01057-25

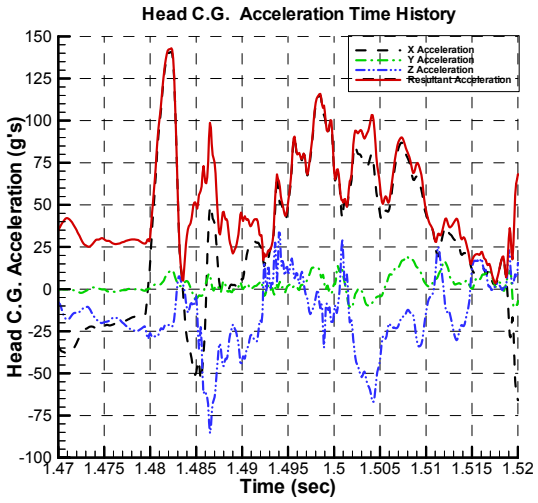

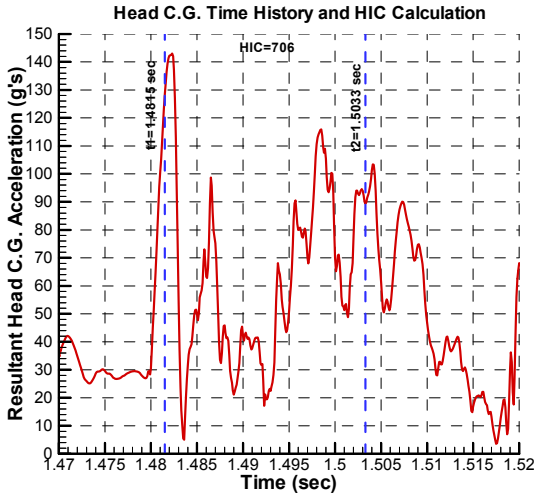

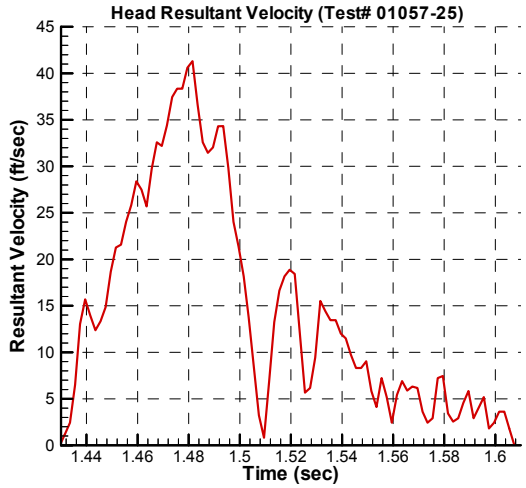

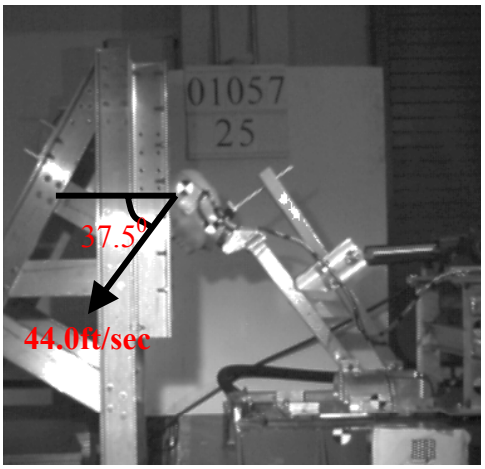

Results of Component HIC Test 01057-25

Bulkhead type	-	0.063-in.-thick Al 2024-T3, 28.5 x 31 in.
Pivot Point setback distance (in.)	-	22.5
Operating Pressure (psi)	-	150
Pendulum Type	-	Al 6061-T6, 7 lbs
Frame Zero (sec)	-	1.6075
Head Impact Velocity (ft/sec)	-	44.0
Head Impact Angle (deg.)	-	37.5
Head c.g. peak resultant accel. (g's)	-	142.9
Head c.g. average resultant accel. (g's)	-	63.9
HIC	-	706
$\Delta t = t_2 - t_1$ (ms)	-	21.8 (t_1 = 1.4815 sec, t_2 = 1.5033 sec)
Contact Start Time, tc_1 (sec)	-	1.4815
Contact End Time, tc_2 (sec)	-	1.5035

DATA FOR HCT TEST 01057-27

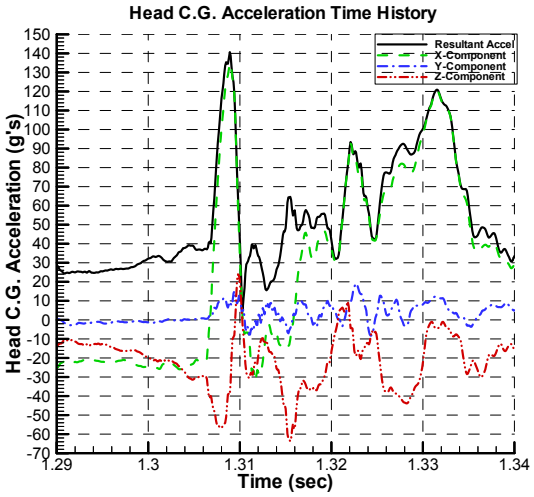

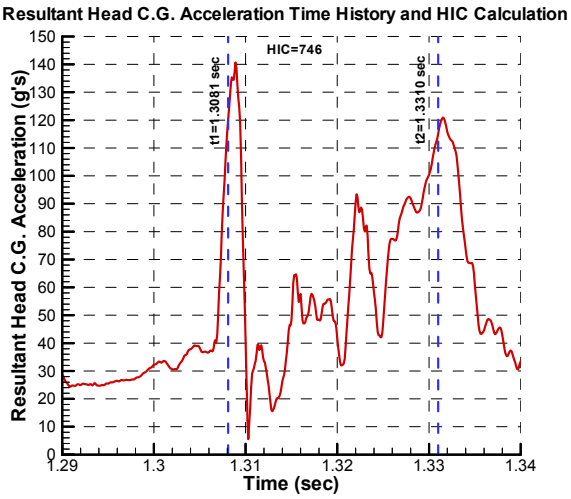

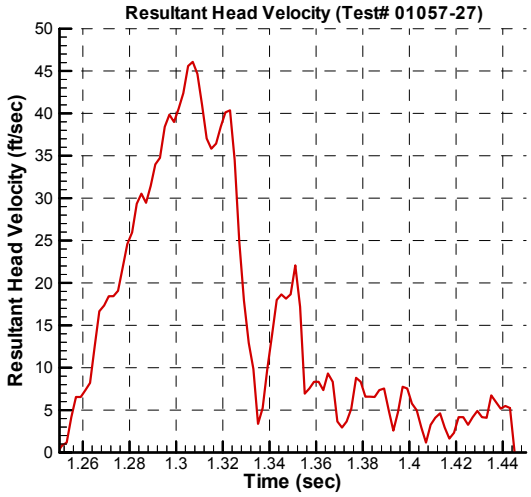

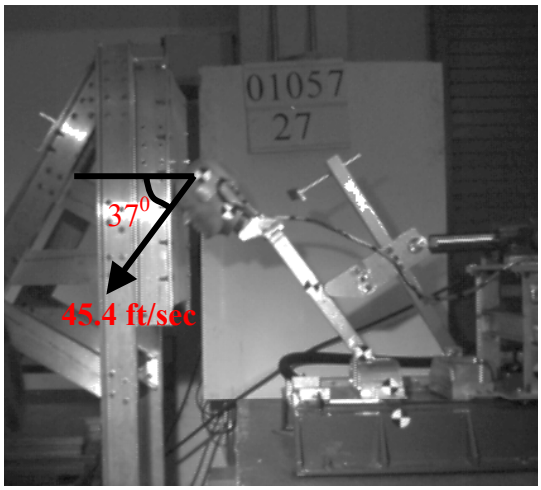

Results of Component HIC Test 01057-27

Bulkhead type	-	0.063-in.-thick Al 2024-T3, 28.5 x 31 in.
Pivot Point setback distance (in.)	-	23.25
Operating Pressure (psi)	-	150
Pendulum Type	-	Al 6061-T6, 7 lbs
Frame Zero (sec)	-	1.4051
Head Impact Velocity (ft/sec)	-	45.4
Head Impact Angle (deg.)	-	37
Head c.g. peak resultant accel. (g's)	-	140.7
Head c.g. average resultant accel. (g's)	-	64
HIC	-	746
$\Delta t = t_2 - t_1$ (ms)	-	22.9 (t_1 = 1.3081 sec, t_2 = 1.3310 sec)
Contact Start Time, tc_1 (sec)	-	1.3081
Contact End Time, tc_2 (sec)	-	1.3311

DATA SHEET FOR HCT TEST 01057-28

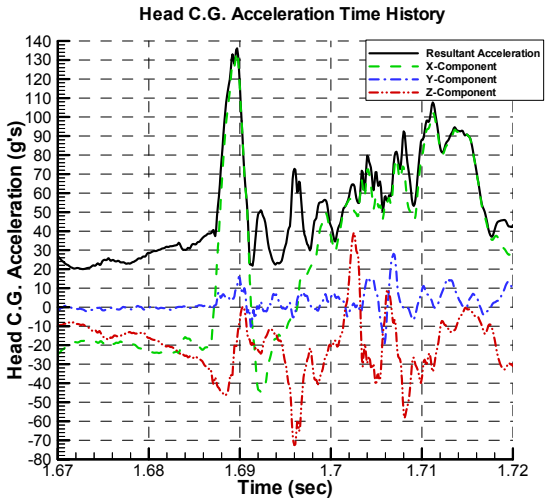

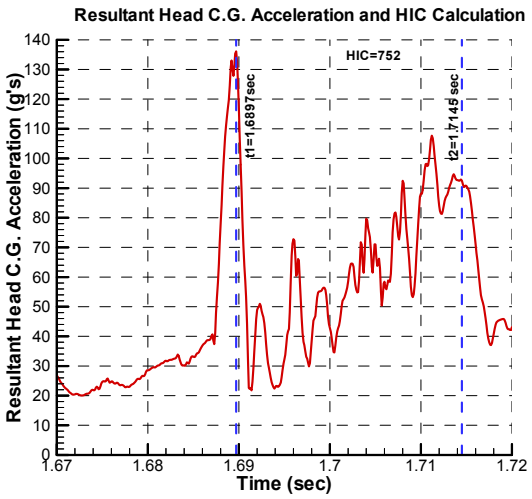

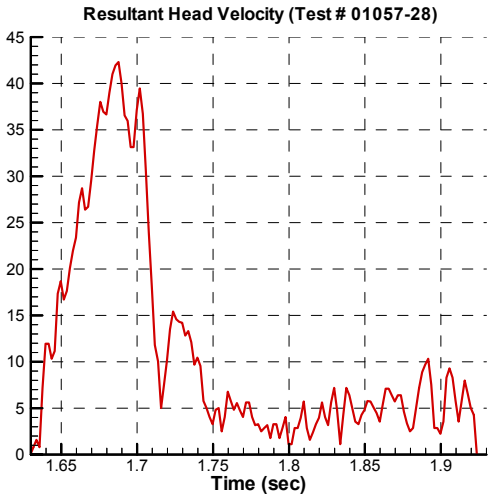

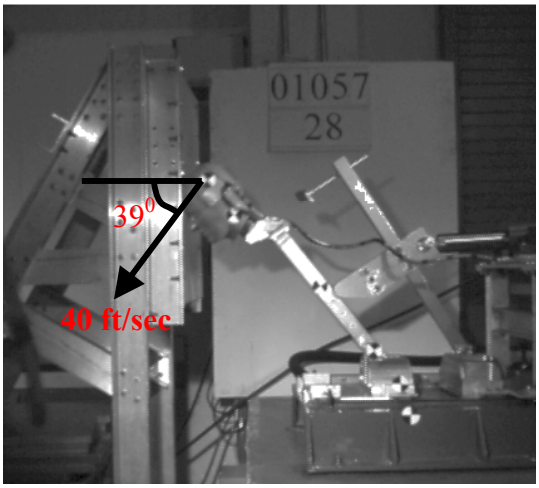

Results of Component HIC Test 01057-28

Bulkhead type	-	0.063-in.-thick Al 2024-T3, 28.5 x 31 in.
Pivot Point setback distance (in.)	-	23.25
Operating Pressure (psi)	-	140
Pendulum Type	-	Al 6061-T6, 7 lbs
Frame Zero (sec)	-	1.8237
Head Impact Velocity (ft/sec)	-	40
Head Impact Angle (deg.)	-	39
Head c.g. resultant peak accel. (g's)	-	136.1
Head c.g. average resultant accel. (g's)	-	62.2
HIC	-	752
$\Delta t = t_2 - t_1$ (ms)	-	24.8 (t_1 = 1.6897 sec, t_2 = 1.7145 sec)
Contact Start Time, tc_1 (sec)	-	1.6897
Contact End Time, tc_2 (sec)	-	1.7147

DATA SHEET FOR HCT TEST 01057-29

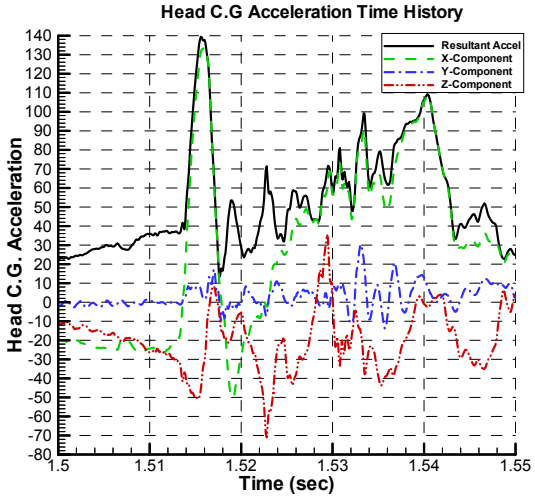

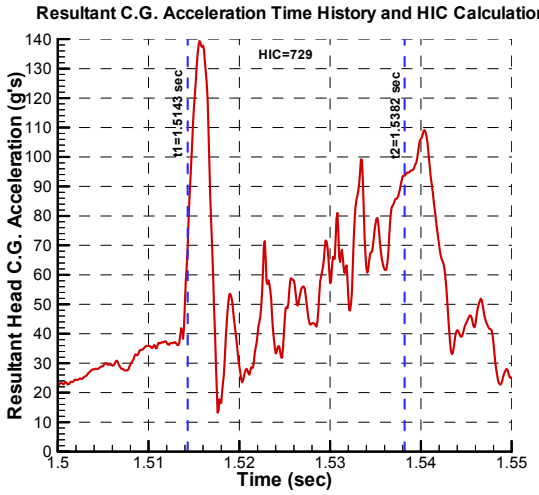

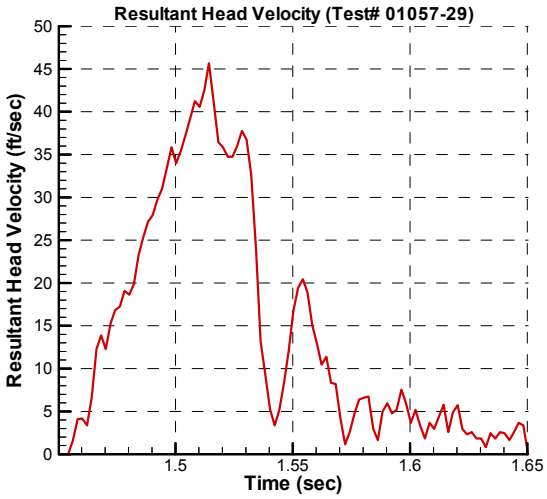

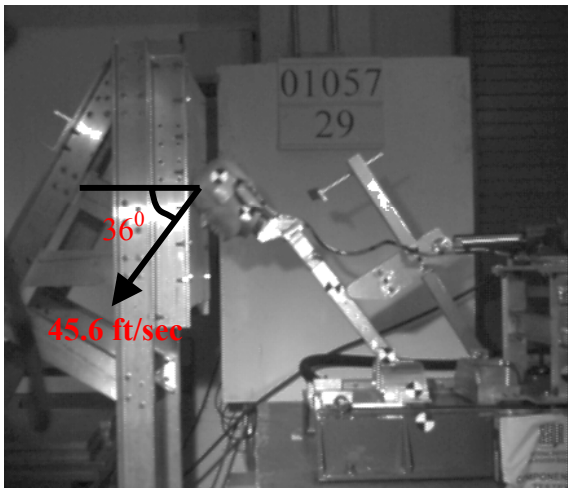

Results of Component HIC Test 01057-29

Bulkhead type	-	0.063-in.-thick Al 2024-T3, 28.5 x 31 in.
Pivot Point setback distance (in.)	-	23.25
Operating Pressure (psi)	-	140
Pendulum Type	-	Al 6061-T6, 7 lbs
Frame Zero (sec)	-	1.5803
Head Impact Velocity (ft/sec)	-	45.6
Head Impact Angle (deg.)	-	36
Head c.g. peak resultant accel. (g's)	-	139.3
Head c.g. average resultant accel. (g's)	-	62.2
HIC	-	729
$\Delta t = t_2 - t_1$ (ms)	-	23.9 (t_1 = 1.5143 sec, t_2 = 1.5382 sec)
Contact Start Time, tc_1 (sec)	-	1.5143
Contact End Time, tc_2 (sec)	-	1.5383

DATA SHEET FOR HCT TEST 01057-43

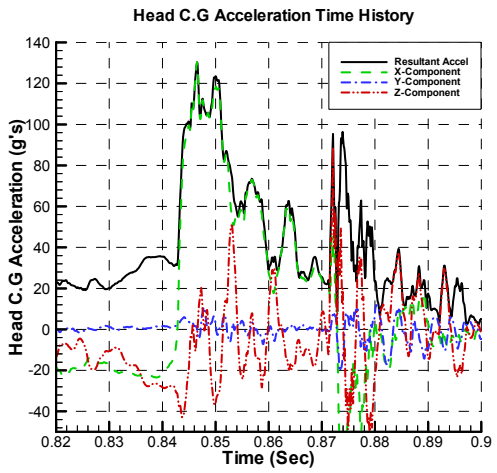

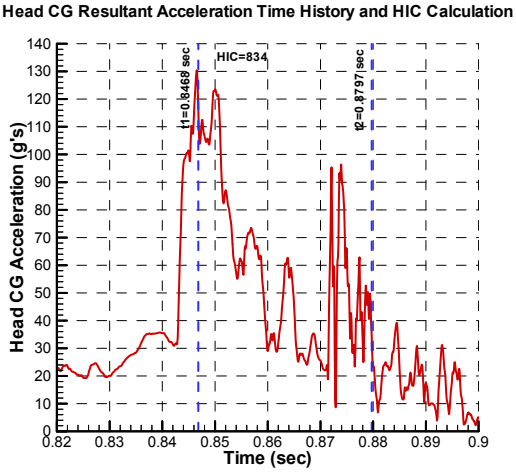

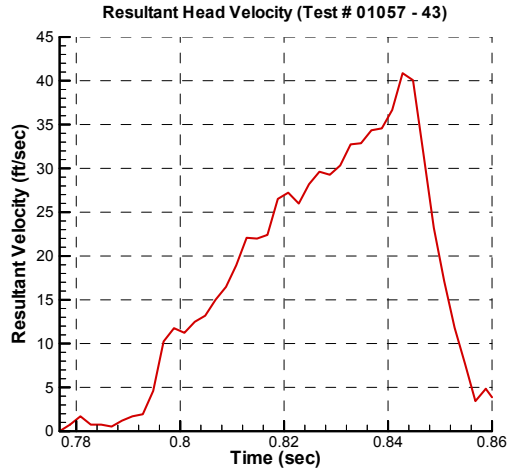

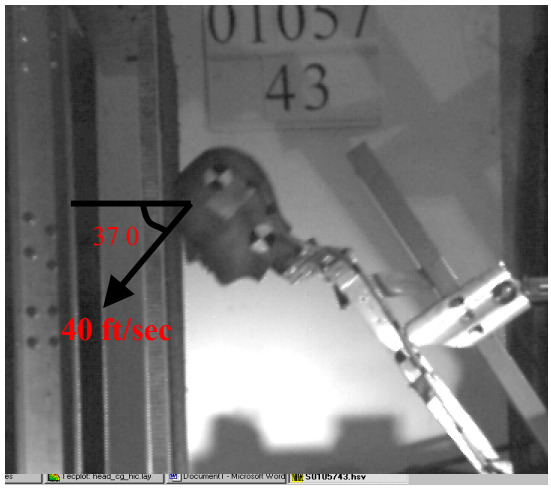

Results of Component HIC Test 01057-43

Bulkhead type	-	Epoxy fiberglass/Nomex honeycomb (1″ thick) covered with carpet
Pivot Point setback distance (in.)	-	23
Operating Pressure (psi)	-	130
Pendulum Type	-	Al 6061-T6, 7 lbs
Frame Zero (sec)	-	0.9368
Head Impact Velocity (ft/sec)	-	40
Head Impact Angle (deg.)	-	37
Head c.g. peak resultant accel. (g's)	-	130.3
Head c.g. average resultant accel. (g's)	-	57.8
HIC	-	834
$\Delta t = t_2 - t_1$ (ms)	-	32.9 (t_1 = 0.8468 sec, t_2 = 0.8797 sec)
Contact Start Time, tc_1 (sec)	-	0.8468
Contact End Time, tc_2 (sec)	-	0.8848

DATA SHEET FOR HCT TEST 01057-44

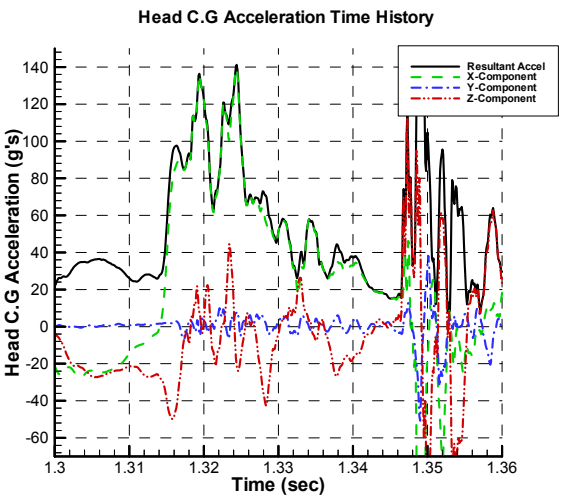

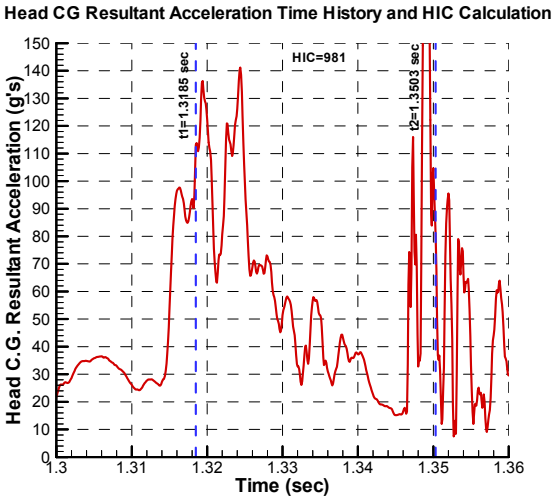

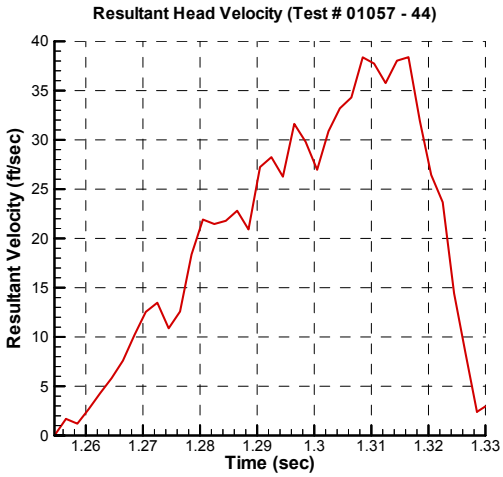

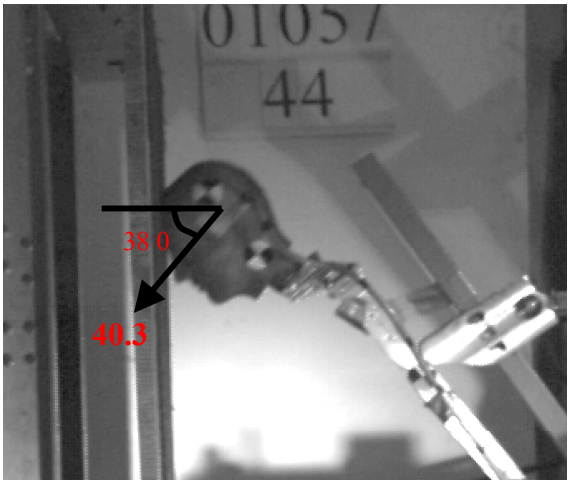

Results of Component HIC Test 01057-44

Bulkhead type	-	Epoxy fiberglass/Nomex honeycomb (1″ thick) covered with carpet
Pivot Point setback distance (in.)	-	23
Operating Pressure (psi)	-	130
Pendulum Type	-	Al 6061-T6, 7 lbs
Frame Zero (sec)	-	1.4245
Head Impact Velocity (ft/sec)	-	40.3
Head Impact Angle (deg.)	-	38
Head c.g. peak resultant accel. (g's)	-	136.3
Head c.g. average resultant accel. (g's)	-	62.6
HIC	-	981
$\Delta t = t_2 - t_1$ (ms)	-	31.8 (t_1 = 1.3185 sec, t_2 = 1.3503 sec)
Contact Start Time, tc_1 (sec)	-	1.3185
Contact End Time, tc_2 (sec)	-	1.3505

DATA SHEET FOR HCT TEST 01057-49

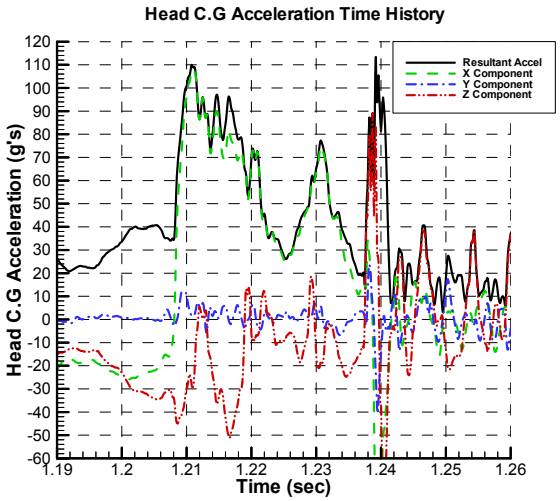

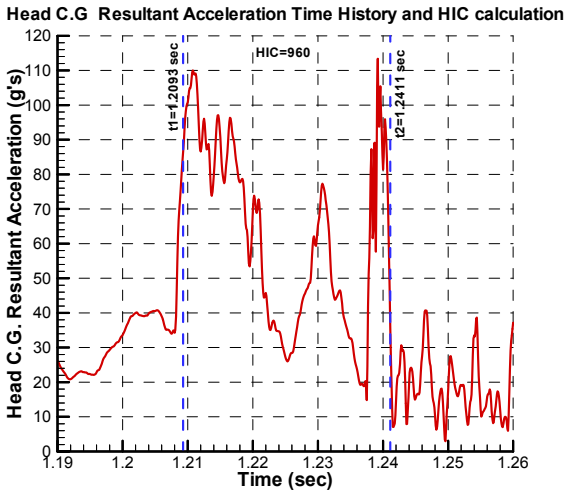

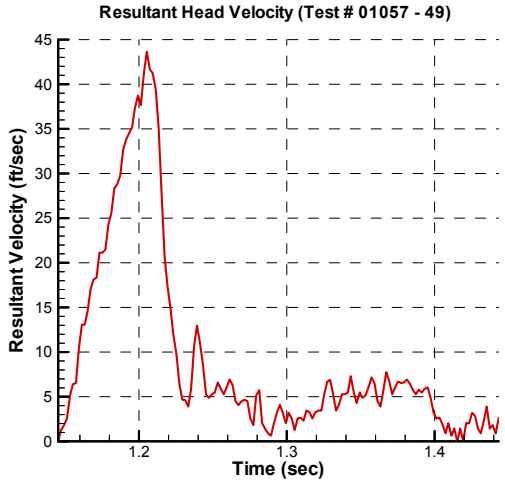

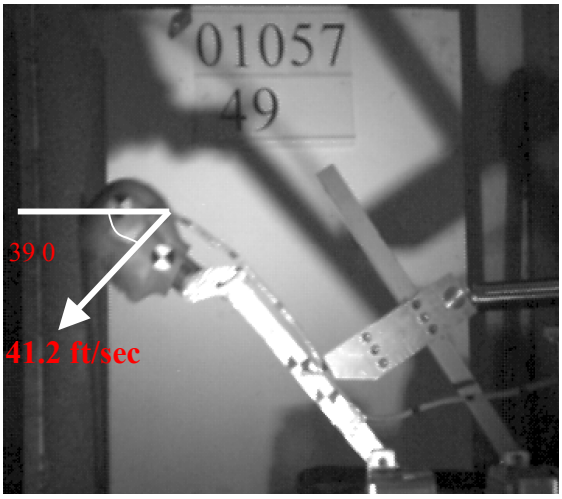

Results of Component HIC Test 01057-49

Bulkhead Type	-	Epoxy fiberglass/Nomex honeycomb (1″ thick) covered with carpet
Pivot Point setback distance (in.)	-	23
Operating Pressure (psi)	-	170
Pendulum Type	-	Al 6061-T6, 7 lbs
Frame Zero (sec)	-	1.3453
Head Impact Velocity (ft/sec)	-	41.2
Head Impact Angle (deg.)	-	39
Head c.g. peak resultant acceleration (g's)	-	109
Head c.g. average resultant accel. (g's)	-	62
HIC	-	960
$\Delta t = t_2 - t_1$ (ms)	-	31.8 (t_1 = 1.2093 sec, t_2 = 1.2411 sec)
Contact Start Time, tc_1 (sec)	-	1.2093
Contact End Time, tc_2 (sec)	-	1.2753